OPTIMIZATION OF VERTICAL AXIS WIND TRUBINE

By:

Adithya Lakkur Venugopal

Ankita Kardile

Matthew Brausch

Sekar Sumanth

MAE598-2016-09

Spring 2016 Final Report

05/02/2016

1. ABSTRACT

Fossil fuels have revolutionized the world for over several decades in the field of power generation. Environmental pollution caused due to conventional sources of energy, have imposed the need to explore alternate, renewable energy sources. Considering the energy crises and pollution problems, ample research with the utilization of Wind energy is being conducted. Arizona has the potential to install up to 10.9GW of onshore wind power generating 30.6TWh annually, however only 238MW wind power nameplate capacity plants have been installed till 2013.

The project focuses on optimizing various design aspects of a vertical axis wind turbine (VAWT) power plant to be able to generate good quality, cheap electricity to satisfy the power demands of the Arizona State University Mesa campus. ASU campus has a solar power generation capacity of 24.1 MW equivalent, however an almost negligible presence of the wind energy source. With an average wind speed of 14.73mph received annually in Mesa, we are trying to tap this potential source of renewable energy. It is anticipated that while trying to minimize the cost of the plant and reduce the payback period, trade-offs will be made to achieve the best possible outcome while maintaining efficiency, safety and quality.

2. TABLE OF CONTENTS

Contents

2.1 List of Tables

2.2 Table of Figures

3. MOTIVATION

With the growing need for sustainable energy, there is the need to optimize the existing options to find the most suitable. Wind turbines offer a method of producing the clean energy, but require careful planning to ensure its success. Optimization of a wind turbine system must take into account the shape of the blades, the structure, the gear train, the materials, and the location.

The team has taken up the optimization of the vertical axis wind turbine (VAWT) in order to set up a wind farm for the ASU campus to meet the rapidly increasing energy requirements and to provide an alternative source of energy. ASU Mesa being a large campus spanning over 592 requires lots of energy and as a result the load on the electricity grid is high. Installation of the wind farm can help ease the load as well as promote renewable energy. Universities such as Notre Dame University and Northern Arizona University have already implemented small scale wind turbines to power the buildings. This further motivated the team to take up this project.

The team choose the VAWT over the Horizontal Axis Wind Turbine (HAWT) for the following reasons:

Horizontal axis wind turbine dominate the majority of the wind industry. Horizontal axis means the rotating axis of the wind turbine is horizontal, or parallel with the ground. Horizontal axis wind turbines are widely used in large scale energy generation. However, in small wind and residential wind applications, vertical axis turbines have their place. The advantage of horizontal wind is that it is able to produce more electricity from a given amount of wind. The disadvantage of horizontal axis however is that it is generally heavier, nosier, requires more place and it does not produce well in turbulent winds. As a result, horizontal axis wind turbine would not be feasible for the ASU campus.

In the Vertical axis wind turbine, the rotational axis of the turbine stands vertical or perpendicular to the ground. As mentioned above, vertical axis turbines are primarily used in small wind projects and residential applications. Vertical axis turbines are powered by wind coming from all 360 degrees, and even some turbines are powered when the wind blows from top to bottom. Because of this versatility, vertical axis wind turbines are thought to be ideal for installations where wind conditions are not consistent, or due to public ordinances the turbine cannot be placed high enough to benefit from steady wind [3.1].

The next important factor to be taken into consideration is the availability of the wind. Based on recent research, the average wind speed required for a feasible wind farm installation in the residential areas is about 10 miles per hour. The team researched on the average wind speeds in the Mesa area with the following results [3.2]:

- Over the course of the year typical wind speeds vary from 0 mph to 16 mph
- The annual average wind speed is about 14.73 mph

Based on the results obtained, the wind speeds are more than the average wind speed required for a feasible wind farm installation.

Taking all the above factors into consideration, the team decided to optimize the wind farm in order to minimize the overall cost which includes the installation cost & material cost. The team has divided the project into 4 sub-systems. They are as follows:

1) Optimal location & positioning of the turbines – Sekar Sumanth
2) Optimal material selection of the turbine blades – Adithya Lakkur Venugopal
3) Aerodynamic optimization of the turbine blades – Matt Brausch
4) Structural optimization of support structure – Ankita Kardile

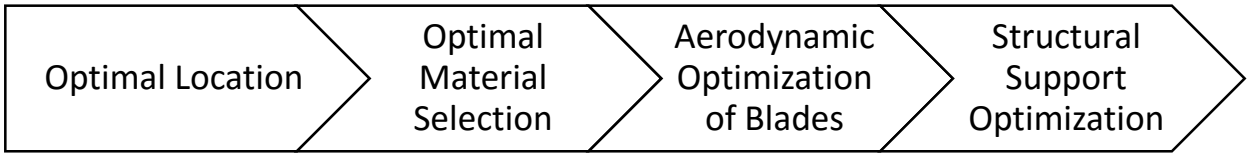

The team aims to identify the optimal location of the wind turbines within the campus and to specifically position the wind turbines together in a particular area to minimize the velocity losses. The turbine blades take up the majority of the cost when it comes to the turbine cost. Hence the optimization of the blade to minimize the weight and in turn minimize the cost. The performance of the turbine depends on the aerodynamic properties of the turbine blades. Hence optimizing the aerodynamics of the blade is of paramount importance. The wind turbine strut is under constant stress leading to generation of the tension & pressure forces along with fatigue. Structural optimization of the strut helps minimize this issue.

4. OPTIMAL POSITIONING OF VERTICAL AXIS WIND TURBINE - SEKAR SUMANTH D

Wind energy, being envisaged as a renewable source of energy, proves to be a clean source of energy. However, it suffers from several constraints for its feasible utility. Arizona State University's commitment to renewable energy and sustainability is evident from its continuous research and development in green sources of energy such as solar energy.

The objective of this section is to intergrade the available data on wind speed and direction in the Mesa area to determine the number of wind turbine per square miles necessary for feasible use of Wind energy in the Arizona State University's campus, which will be useful in determination of optimal positioning of the wind turbines in the wind farm.

An effort has been made in this section to optimize the positioning of given vertical axis wind turbines in a given wind farm. MATLAB's 'fmincon' optimizer tool was used to solve the optimization problem. The results from this study will be further used to integrate the optimization study from other sections of this project, to optimize the cost of installation of vertical axis wind farm in ASU's campus.

Essentially the wind turbines are classified into horizontal axis and vertical axis wind turbines. There are several constraints for positioning of a wind turbine in a wind farm. Some of the prominent ones are as follows

- Access for maintenance
- Wind speed
- Wind direction
- Closeness to the electrical grid
- Space and size constrained

Further there are various factor that influence the location of a wind farm are as follows

- Hourly load demand for a micro grid vs the peak load demand
- Hourly wind speed pattern of a particular area
- Wind direction pattern
- Seasonal pattern

This section of the optimization study is based on the data analysis from the data acquisition system at ASU's Polytechnic campus to determine the optimal positioning of vertical axis wind turbines in a wind farm.

4.1Nomenclature

N	=	Number of wind turbines
u	=	Velocity in the wake of a wind turbine
U	=	Free stream velocity
a	=	Axial induction factor
x	=	Downstream distance from the wind turbine
r_r	=	Rotor radius of the wind turbine
r_o	=	Radius of the wake
d_r	=	Wake radius at the downwind plane of the wind turbine
z	=	Hub height of the wind turbine
Z_o	=	Surface roughness height of the site
η	=	Efficiency of the wind turbine
ρ	=	Air density
α	=	Entrainment Constant

4.2 Mathematical Model

The main purpose of this study is to maximize the power output from the given windfarm. Therefore it is necessary to model the positioning of the Vertical axis wind turbines in a given farm to maximize the yield.

For the purpose of this study a wake and power analysis on a Vertical Axis wind turbines using a simple wake model is employed.

It is important to note that a wake is always generated at the vicinity of a given Wind turbine. Our goal is to determine this wake region and its effects on the wind turbine placement. According to

the Jensen's wake modelling of Horizontal axis wind turbine [4.1], the velocity of the wind in the wake region at a distance x downstream of the turbine can be determined using the principle of conservation of momentum. A similar principle can be adopted for the Vertical axis turbine's analysis with a slight modifications.

4.2.1 Wake Model for Vertical Axis Wind Turbine

Let ***U*** be the mean free stream wind turbine. Then for a rotor radius of the turbine r_r, the velocity of the wind in the wake region at a distance ***x*** from the center of the turbine is given by the following formula:

$$u = U[1 - \frac{2a}{1+\alpha(x/r_0)}]$$, modified the Jensen's model [4.1] *Equation (1)*

Here the value of ***a***, which is the axial induction factor for a single stream tube model for a two dimensional single straight blade vertical axis wind turbine is given by the formula[4.2]

$$a \approx \frac{1}{16}\frac{Bc}{R}eC_{l,\alpha}\lambda$$ *Equation (2)*

Where,

- *B* is the number of blades
- *c* is the chord length of the blade airfoil
- $C_{1,a}$ is the lift curve slope for small angles of attack[1]
- *R* is the rotor radius
- λ is the tip speed ratio

The value of the entrainment constant ***α*** for a given hub height of the turbine ***(z)*** and surface roughness factor (z_0) can be determined by the formula [4.3]:

---

[1] The value of $C_{1,a}$ is calculated from the lift vs. angle of attack curve for NACA0015 from NACA report where it is consider equal to value of (18/π)

$$\alpha = \frac{0.5}{\ln(z / z_0)}$$ *Equation (3)*

The optimal values of these parameters were determined from the optimization studies in the next sections of this project.

It is important to note that this formula was derived considering the horizontal axis wind turbine. Therefore, it is necessary to modify the entrainment constant formula for the purpose of Vertical axis wind turbine. The value of hub height of the turbine ***(z),*** has to be equated to that of the Height of the wind turbine

The same formula can be used for the Vertical axis turbines as well, except that the hub height has to be replaced by the height of the turbine *(H).*

4.2.2 Power Model for a vertical axis wind turbine [4.8]

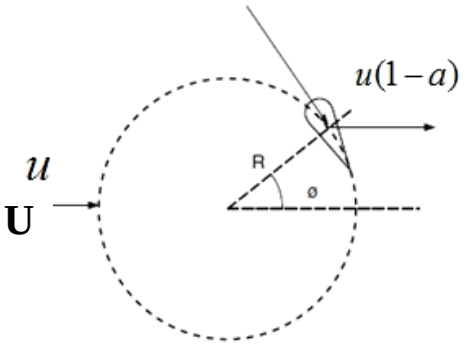

FIGURE 1: SINGLE STREAM TUBE GEOMETRY OF A VAWT

It is assumed that for vertical axis wind turbine to be an actuator disc, due to which the near field effect behind or to the sides of the turbine is neglected [4.1]. The power output from a single vertical axis wind turbine can be determined using the following formula:

$$P_s = \frac{1}{2}\rho(2RH)U^3 C_p$$ *Equation (4)*

Therefore, the total power from the wind farm can be obtained by multiplying the above equation with the number of turbines *N*.

The coefficient of power *Cp* can be determined using the formula from the book of by Manwell, McGowan and Rogers for wind turbine [2]

$$C_p \approx 4ea(1-a)^2 - \frac{1}{2}\frac{Bc}{R}C_{d,0}\lambda^3 \qquad \textit{Equation (5)}$$

Where, the value of *e* is the ratio of velocity of in the wake *u* with respect to free stream velocity *U*. Further, the value of $C_{d,0}$ is assumed to be zero.

For wind turbines arranged one behind the other or which are close to the vicinity of another turbine, the mean velocity of wake can be calculated using the equation 1. Similarly, for the entire wind farm the mean velocity of the wake is determine using the equation 1.

4.2.3 Objective function

Therefore, the objective function reduces to minimizing the value of ***x*** (the distance at which turbines has to be place), with respect to Ps and N.

4.2.4 Constraints

Number of turbines: The number of turbine required in the wind farm is taken as one of the constraints.

Total Power: Total power output required from the plant is considered as another constraints

Axial induction factor: The axial induction factor is take as the third constraint.

The result of from this minimization problem will provide the minimum distance required to effectively position the turbines without being influenced by the wake.

4.2.5 Assumptions

- The optimization calculations are carried considering a fixed wind speed.
- The ratio of mean wind speed in the wind farm's wake region to the free stream wind speed is considered as a constant for particular free stream velocity.
- Wind turbines are arranged one behind the other or one adjacent to another along a specific row or column in the wind farm
- Efficiency of the turbine is assumed to be common for all the turbines
- One directional wind flow is assumed.

- Near field effect of the turbine with the direction of the wind is ignored as it is considerably low[4.1]

4.3 Model Analysis

4.3.1 Preliminary wind analysis

4.3.1.1 Wind speed analysis

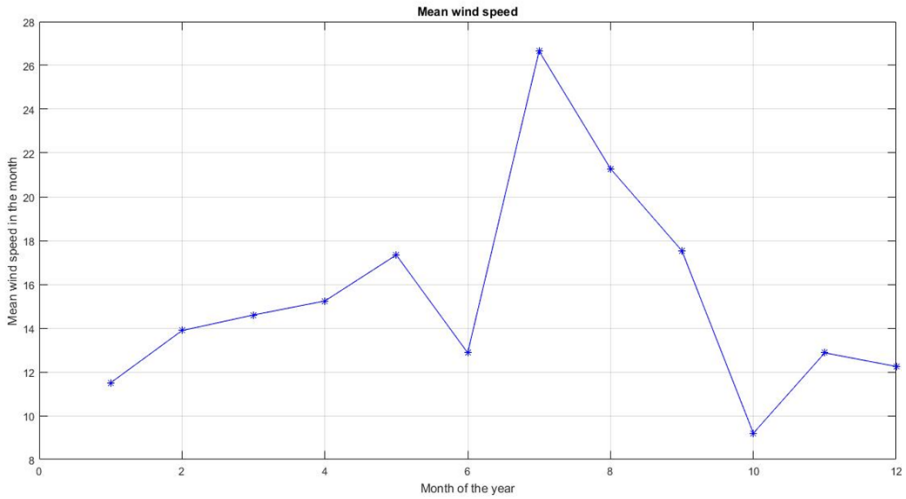

FIGURE 2: PLOT OF WIND SPEED VS MONTH OF THE YEAR

Optimization of the wind farm and wind turbine essential requires an analysis of the wind pattern in the area that the wind turbines are meant to be erected.

Over a preliminary analysis of the Wind speeds from a Data acquisition system at ASU's Polytechnic campus, it was found that the maximum mean wind speed was 27mph. Therefore, the turbine has to be designed for speeds equal to or higher than this speed.

4.3.1.2 Wind direction analysis

It is essential to study the wind direction pattern. Similarly an analysis was performed on the raw data from the data acquisition system at Polytechnic's campus. The figure shows the distribution of wind in the Mesa County based on the analysis of raw data.

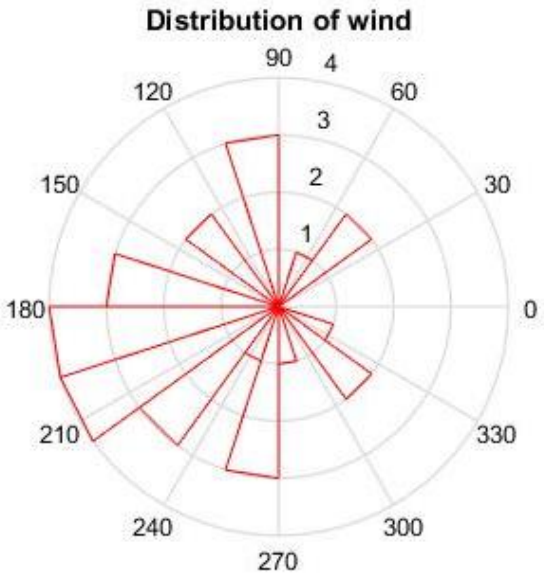

FIGURE 3: REPERSENTATION OF WIND DIRECTION

It can be noted that maximum wind distribution is along North to South direction at an angle of 180 to 210 Degrees with respect to the North.

Therefore, the wind turbines has to be placed along this direction of Wind. However, for our consideration the direction is assumed to be fixed. Also, it can be highlighted that the direction of the wind has considerably less effect on power generation for a Vertical axis wind turbine compared to that of the Horizontal axis.

4.3.2 Monotonicity Analysis

The minimization problem of the distance between the turbines can be reduced from the Power equation.

Consider the power equation (equation 4):

$$P_s = \frac{1}{2}\rho(2RH)U^3 C_p$$

The total power required from the wind farm can be obtained by multiplying the above equation with N, the number of turbines to be erected.

$$C_p \approx 4ea(1-a)^2 - \frac{1}{2}\frac{Bc}{R}C_{d,0}\lambda^3$$

The coefficient of power *Cp* given by the above equation is plugged into the power equation. It is considered that $C_{d,0}$ as zero [4.6]

Re-writing the equation and substituting the values of *Cp* we get the following, we can derive the required objective function.

Objective Function

Function (x): (r0 [1- (NηρH4a (1-a)^{2}U^3-Ps)]) / 2αa

This objective function has to be minimized with respect to N, P_s and a

Problem Constraints

Inequality constraints

G1: *From cost function equation*

We consider the Cost of operating the turbine equation. This equation has to be subtracted from ratio of the available cost for maintenance of the wind turbine/ hour and the total power output from the wind farm. This has to be less than or equal to zero.

$$cost = N(\frac{2}{3} + \frac{1}{3}e^{-0.00174N^2})$$

Therefore,

G1: (Cost of operating the turbine/Hour) – N ((2/3) + (1/3) e$^{-0.00174N2}$) ≤ 0

G2: *From Axial induction factor equation*

We consider the axial induction factor *a*. The value of *a* has to be less than or equal to zero for the adjacent turbine's optimal performance [4.1]. Therefore, from equation (3) we can deduce the next inequality constraint as follows:

G2: a – (B c e 18 λ)/1πR

Equality constraints

H1: The equality constraint can be deduced from the Coefficient of power equation and from the total power output relation with the wind speed loss factor [4.3]

$$P_{tot} = \Sigma\ 0.3\ u\ (1-a)$$

Reducing the equations we get

$$H1: N - [P_s a\ (1-a)^2] = 0$$

Parameters:

For the optimization analysis the following parameters were considered based on the design optimization results from the next study of this project:

- B is the number of blades = 4
- c is the chord length of the blade airfoil = 0.5 m
- $C_{1,a}$ is the lift curve slope for small angles of attack[2] = $18/\pi$
- R is the rotor radius = 1.5626 m
- λ is the tip speed ratio = 0.76
- Cost of operating the turbine per hour = 40 USD
- Efficiency of the turbine = 70%
- Ratio of mean wake speed to mean wind speed = 0.85 (Assuming there is 15% loss)

[2] The value of $C_{1,a}$ is calculated from the lift vs. angle of attack curve for NACA0015 from NACA report where it is consider equal to value of $(18/\pi)$

TABLE 1: MONOTONICITY TABLE

	N	Ps	a
f	+	+	+
G1	-	-	
G2	+	+	+

Therefore, G1 is an active constraint as seen from Monotonicity Principle 1. Also it can be seen that the problem is well bounded.

4.4 Optimization Study

4.4.1 MATLAB Modeling

The fmincon solver of the Matlab was is used for the optimization study. The interior point algorithm is used for this purpose. The codes in APPENDIX A were developed in Matlab for the optimization analysis.

4.4.2 MATLAB Results

Case 1: Mean wind speed

U = 26.5 mph

lb = [0,0,0];

ub = [100 100 100];

x0 = [63,100,1];

```
Local minimum possible. Constraints satisfied.

fmincon stopped because the size of the current step is less than
the default value of the step size tolerance and constraints are
satisfied to within the default value of the constraint tolerance.

xopt =

    1.9257   15.4424    0.2961

exitflag =

     2

output =

         iterations: 32
          funcCount: 186
    constrviolation: 3.6660e-06
```

```
          stepsize: 4.0053e-10
         algorithm: 'interior-point'
     firstorderopt: 9.1688e+06
      cgiterations: 28
           message: 'Local minimum possible. Constraints satisfied....'
```

```
minimum required x value =

  112.9954 m
```

Published with MATLAB® R2015b

Case 2: Maximum Wind Speed for which the turbine is designed

U = 50 mph

lb = [0,0,0];

ub = [100 100 100];

x0 = [63,100,1];

```
minimum required x value =

  759.048 m
```

Published with MATLAB® R2015b

Case 3: Minimum Wind Speed for Sufficient Power generation

U = 10 mph

lb = [0,0,0];

ub = [100 100 100];

x0 = [63,100,1];

```
minimum required x value =

  58.61 m
```

Published with MATLAB® R2015b

4.4.3 Conclusion from MATLAB Results

From the wind data analyis it is known that the mean wind speed is roughly in the range of 20-26.5 Mph throughout the year therefore, the minimum diplacement between the turbines are considered to be 112.9954 Meters for the wind farm's optimal performance.

Therefore from the optimization results it can be noted that for a wind speed of 26.5 Mph, a minimum of two turbines are required to produce a net power output of 15 Kilowatt. The minimum displacement between the two wind turbine is 112.951m.

It can be noted that with the increase in Wind speed the distance required inbetween the turbines, to avoid interference with the Wake region also increases. This proves that the distance between the turbines has to be chosen accordingly to the situations at which the wind farm is designed.

4.5 Discussion of Results

4.5.1 Layout of the Wind Turbine Placement in the Wind Farm

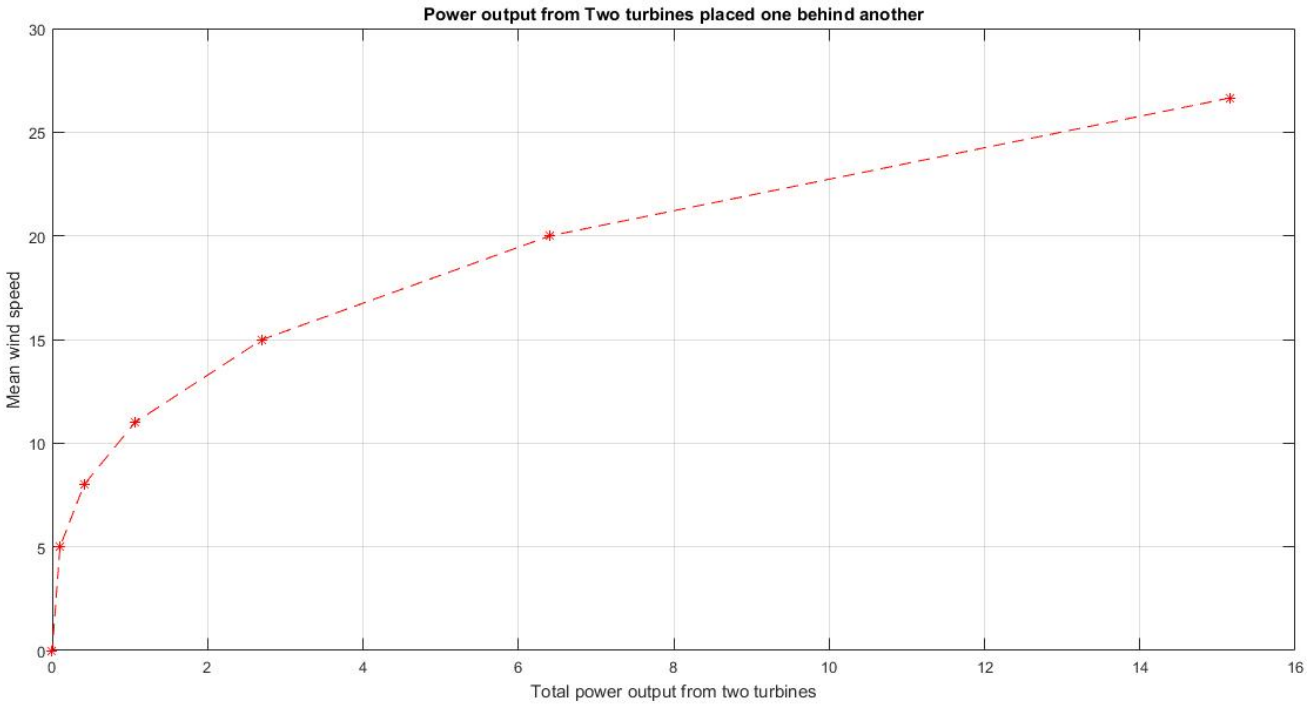

FIGURE 4: PLOT OF WIND SPEED VS POWER OUTPUT

4.5.2 Relation of Power with Wind Velocity

A plot of Total output Power in Kilo Watt from two wind turbines vs wind speed for specific dimensions of the wind turbines based on the next optimization study was considered and the output power was plotted for the range of wind speed data which was noted by the data acquisition system. It can be inferred from the plot that for the mean wind speed of 26.6 Mph, for which this optimization algorithm was developed the output power is approximately 15KW. This verifies the suitability of algorithm developed for the situation considered.

Thus with the increase in wind speed the net power output from the turbine should increase exponentially for the range of speeds the wind turbines are designed for.

This proves that the wind turbines has to be placed in the direction of maximum mean wind speed.

4.5.3 Wind Turbine Placement Model

The Vertical Axis Wind turbine does have an advantage in dealing with wind direction shifts. Therefore, it is easier to design a Vertical axis wind turbine farm compared to that of Horizontal axis wind turbine farm. For the purpose of modeling we consider the optimal layout proposed by Grady et al.[4.4] CFD analysis for Vertical axis wind turbine analysis and use the values of distance between turbines from the result of our optimization problem. Therefore, irrespective of the wind direction shift the Net power output from the wind farm should theoretically[4.8] be same in all the cases.

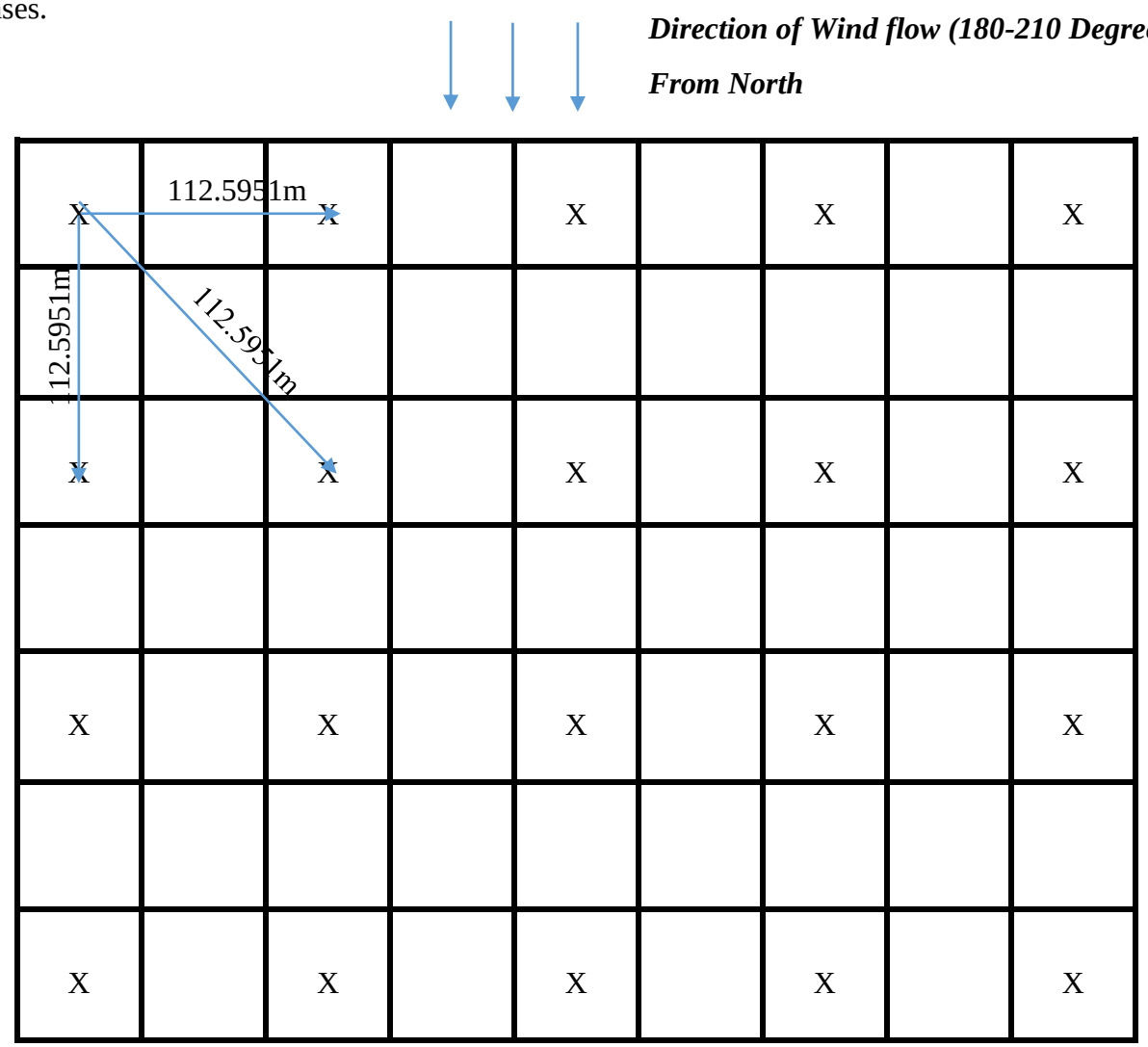

FIGURE 5: PLACEMENT OF THE WIND TURBINES IN THE WIND FARM

Therefore by increasing the size of the wind farm, there should be a corresponding increase in Total Power output from the farm. However, this will trade off with the cost of maintenance of the wind farm.

4.5.4 System Tradeoffs

Distance between Turbines [X &Y direction]

It is important to highlight that the wake region increase with the increase in wind speed. Therefore, the value of the distance between the turbines should increase with increase in wind speed. This can be seen from the results from the analysis.

Thus, the distance between the turbines has to be chosen appropriately for the wind speeds for which the wind farm operates.

This ensures, that the wind turbines are not placed in the wake region for maximum power output.

Elevation of the Turbines [Z direction]

The situation considered ignores the fact that the elevation of location of wind turbine plays a vital role in the power output. With the increase in elevation there should be a corresponding increase in mean wind speed, and thus more is the distance of spacing required in between the turbines.

Number of Turbines

For the case that this optimization study has considered it is assumed that the mechanical and power transmission efficiency to be same for all the turbines and the efficiency of the wind farm has been ignored. However, the efficiency of the wind turbines are influenced by various factors. Further, the efficiency of the wind turbines near the wind flow direction is more compared to those away from the wind flow, simply because of the wind loss factor.

5. MATERIAL SELECTION OF TURBINE BLADES – ADITHYA LAKKUR VENUGOPAL

A composite material can be defined as a material that is made up of 2 or more constituent materials with varying properties which, when combined leads to a composite material having distinctive properties when compared to the original materials.

Selection of materials for a composite structure requires consideration of much more than properties in a table. Selection of the fiber, the form in which the fiber is to be used, and the matrix material involves many factors such as [5.1]:

- Structural performance
- Shape of the product
- Environmental conditions, e.g., fatigue, Temperature, humidity, corrosives
- Number to pieces to be produced

The wind turbine blade is specifically made from laminated composite materials because of properties such as low density, excellent mechanical properties, good corrosion resistance, and tailor-ability of the properties and the diversity of fabrication. All these properties make composite materials suitable for wind turbine blades. [5.2]

2 composite materials selected for the wind turbine blades are:

- Glass reinforced plastic
- Carbon filament reinforced plastic

Problem Statement

The main design goal is to select the best material and to minimize the mass of the turbine blade for the vertical axis wind turbine (VAWT) based on the organization of matrix and reinforcement to optimize properties for application. This leads to the reduction in cost which is the overall objective. In the case of turbine blades, low density and high strength are the required properties [5.3].

5.1 Nomenclature

Vm	=	Volume fraction of the matrix (%)
Vf	=	Volume fraction of the fiber (%)
ρm	=	Density of the matrix (kg/m3)

ρf	=	Density of the fiber (kg/m3)
E1	=	Longitudinal young's modulus (MPa)
E2	=	Transverse young's modulus (MPa)
G12	=	Rigidity modulus (MPa)
c_c	=	Cost of the composite (per kg)
m_f	=	Mass of the fiber (per kg)
T_c	=	Thickness of the composite (mm)
T_p	=	Thickness of the foam (mm)
T_r	=	Thickness of epoxy resin (mm)
σ_{PVC}	=	Max stress of PVC foam (MPa)
t	=	Thickness of the laminate (m)
ν	=	Poisson's ratio
d	=	Deformation in the blade (mm)

5.2 Mathematical Model

5.2.1 Turbine Blade Materials

Based on the operational parameters and the surrounding conditions of a typical VAWT for delivering electrical or mechanical energy, the following properties of the VAWT blade materials are required [5.4]:

- It should have adequately high yield strength for longer life;
- It must endure a very large number of fatigue cycles during their service lifetime to reduce material degradation;
- It should have high material stiffness to maintain optimal aerodynamic performance;
- It should have low density for reduced amount of gravity and normal force component;
- It should be corrosion resistant;
- It should be suitable for cheaper fabrication methods;
- It must be efficiently manufactured into their final form;
- It should provide a long-term mechanical performance per unit cost;

Hence it is important to optimize the mass of the composite material that facilitates in obtaining the desired properties. There exists a trade-off between the turbine blade mass and the power generation. Heavier the turbine blade, the heavier the turbine tower and this leads to complications

such as installation difficulties, power losses, maintenance issues, safely issues & feasibility of the wind turbine [5.5].

The foam is used as the core and the reinforcing material is laid over the form there by forming a strong material with suitable properties. The 2 materials selected for the optimization study along with the form are as follows [5.6]:

- Glass reinforced plastic
- Carbon filament reinforced plastic
- PVC Foam 60 kgm^3

5.2.2 Objective function

The objective function for this problem will be to minimize the mass of the turbine blade. The mass of the blade depends on the volume fraction of the fiber & matrix, thickness of the composite, density of the composite and number of stacks of the ply system.

The composite materials selected have varying mechanical properties that depend on all the above factors. As a result, the material that satisfies all the above requirements with the least weight will be selected as the optimized solution.

Minimize $$T_c = T_f + T_m \quad \textbf{[Eq. 5.1]}$$

Based on the optimized thickness, the cost of the composite material is calculated using the below equations [5.7]

$$\bar{c}_c = \bar{m}_f \bar{c}_f + (1 - \bar{m}_f)\bar{c}_m \quad \textbf{[Eq. 5.2]}$$

$$\bar{m}_f = \frac{s_f}{s_c}\left(\frac{v_f}{v_c}\right); \quad \bar{m}_m = 1 - \bar{m}_f \quad \textbf{[Eq. 5.3]}$$

As the mass of the composite reduces, the cost of the composite reduces. This trade off benefits the overall objective to reduce the mass of the blade.

5.2.3 Assumptions

- The laminate system is symmetric
- Unidirectional fibers are used for the layup
- Thickness of each ply is fixed
- There is no moment experienced by the laminate

- The layers of the laminate is assumed to be perfectly bonded
- Linear elastic behavior
- Plane sections normal to the longitudinal axis remain plane and normal during bending
- Quasi – isotropic layup of plies is considered
- Fiber volume (v_f) of 0.55 is used for the composite material

The plies of a quasi-isotropic layup are stacked in a 0°, –45°, 45°, and 90° sequence or in a 0°, –60°, and 60° sequence. These ply orientations simulate the properties of an isotropic material. [5.8]

5.2.4 Constraints

There are several constraints to be taken into consideration during the optimization. There are limiting values for properties that we must define in order to solve the problem.

5.2.4.1 Young's modulus of the composite material (**E_1, E_2**)

Composites materials are known for their tailor-ability to obtain the desired properties. Based on the fiber volume fraction, the properties of the composite can be changed. Moreover, the properties along the longitudinal (E_1) & transverse direction (E_2) also vary drastically especially in unidirectional composites. As a result, the Young's Modulus of the composite is one of the major constraints. To calculate the Young's Modulus, the following equations are made use. [5.7]

$$E_1 = (E_m * v_m) + (E_f * v_f) \qquad \textbf{[Eq. 5.4]}$$

$$E_2 = 1/((v_m/E_m) + (v_f/E_f)) \qquad \textbf{[Eq. 5.5]}$$

5.2.4.2 Rigidity modulus of the composite material (**G_{12}**)

Similar to the Young's Modulus of the composite, the Rigidity Modulus also changes with the change of fiber volume fraction. Rigidity modulus is basically the ability of the material to resist the transverse deformations in the composite material. Since the blade experience's a load from all directions, the shear properties come into play. The Rigidity Modulus of the composite material is calculated using the following equation. [5.7]

$$G_{12} = 1/((v_m/G_m) + (v_f/G_f)) \qquad \textbf{[Eq. 5.6]}$$

5.2.4.3 Density of the composite material (**ρ_c**)

The density of the composite material plays a very important role as it is directly proportional to the weight of the material. The density of the composite material is based off the fiber volume

fraction and as a result needs to be calculated and constrained. The density of the composite is calculated using the following equation. [5.7]

$$\rho_c = (\rho_m * v_m) + (\rho_f * v_f) \quad \textbf{[Eq. 5.7]}$$

5.2.4.4 Maximum stress of the PVC Foam ($\boldsymbol{\sigma_{PVC}}$)

The maximum stress that the PVC Form can take acts as the limiting factor as it leads to the failure of the blade. The PVC Foam has a yield stress of 65 MPa.

$$\sigma_{PVC} = 65 \text{ MPa} \quad \textbf{[Eq. 5.8]}$$

5.2.4.5 Maximum deformation of the blade (**d**)

The blade is subjected to various stresses and as a result the structural integrity of the blade must be maintained. Thus the deformation of the blade also acts as another constraint.

5.2.5 Design Variables and Parameters

5.2.5.1 Design Variables

The design variables are the defining factors for any optimization problem. The variables help us formulate the objective function.

The materials for the turbine blade as discussed in the previous sections are carbon fiber and EGlass fiber. It's of paramount importance for the cost of the turbine blade to be minimum. The dictating factor for the material cost is the amount of fiber and resin used for the layup i.e. the thickness of the composite laminate. Based on the laminate thickness, the mass of the composite can be calculated which in-turn gives us the cost of the turbine blade.

The properties of the carbon fiber, EGlass and epoxy resin are as shown in the table below.

TABLE 2: PROPERTIES OF THE COMPOSITE MATERIALS

Property	Carbon Fiber	EGlass Fiber	Epoxy Resin
Density, ρ (kg/m^3)	1740	2575	1250
Young's Modulus, E (GPa)	276	72.4	3.2
Rigidity Modulus, G (GPa)	18	33	1.02
Cost per kg ($)	88	12	22

As discussed in the previous section, the fiber volume fraction of 0.55 was assumed for the analysis. The properties of the composite materials were calculated using the equations by utilizing the MATLAB code in APPENDIX C.

TABLE 3: PROPERTIES OF THE COMPOSITE MATERIALS AT 0.55 FIBER VOLUME FRACTION

Property	Carbon-Epoxy Composite	EGlass-Epoxy Composite
Density, ρ (kg/m^3)	1490	2000
Young's Modulus, E_1 (GPa)	201	65
Young's Modulus, E_2 (GPa)	8.6	10
Rigidity Modulus, G_{12} (GPa)	4.7	13
Cost per kg ($)	94	32

We can clearly see that the properties of the composite material varied drastically when determined using the above equations. The above properties will be used during the analysis of the turbine blade.

In this subsystem, the variables that are most important are as follows:

- Thickness of the PCV Foam (**T_p**)
- Thickness of the epoxy resin (**T_r**)
- Thickness of the fiber (**T_f**)

We can clearly see that the laminate thickness is dependent of the above mentioned material thickness.

5.2.5.2 Parameters Set

The following parameters are used to perform the analysis using the ANSYS Workbench simulation tool.

- Foam Thickness
- Fiber Thickness
- Epoxy Thickness
- Maximum Equivalent Stress
- Total Deformation
- Laminate Thickness

5.2.6 Summary Model

Minimize

$$T_c = T_f + T_m$$

Subject to

$$\sigma_{max} \leq 65 \text{ MPa}$$

$$d \leq 2 \text{ mm}$$

5.3 ANSYS Simulation

The material which provides the best structural properties and at the same time minimizes the cost will be selected as the best material. The ANSYS Composite PrePost (ACP) module of the ANSYS Workbench was used for the analysis since the material in study is composites. [5.9]

A typical turbine blade is made up of a core made up of a foam and the reinforcing material is laid around the foam. The same procedure was followed for the analysis. The core was placed and the composite material was laid over it.

5.3.1 Workbench setup

The static structural module was used to perform the loading on the turbine blade as shown in **figure 6**.

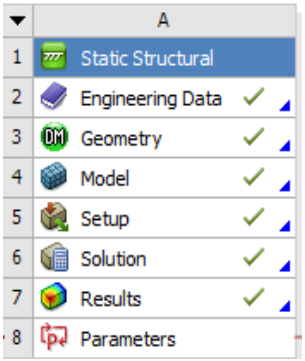

FIGURE 6: STATIC STRUCTURAL MODULE

The 'Engineering Data' tab was selected and the materials properties calculated in section 2.2.5.1 were given as the inputs.

The new materials defined are as follows:

- Core – PVC Foam 60 kgm^3
- Resin – Epoxy
- Fiber – Eglass/ Carbon fiber

5.3.2 Geometry of the turbine blade

The ANSYS DesignModeler was used to construct the turbine blade. A rectangular cross section of the blade was considered for the simulation as it best represented the turbine blade of the vertical axis wind turbine. The rectangular c/s also helped simplify the composite layup process. The dimensions of the turbine blade are as follows:

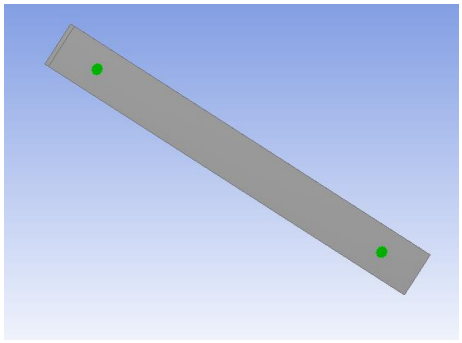

FIGURE 7: TURBINE BLADE WITH STRUT LOCATION

TABLE 4: BLADE DIMENSIONS

Height	1.5 m
Chord length	0.4 m

Figure 7 shows the turbine blade along with strut positions. The turbine blade is attached to the central hanger using the strut. The strut is riveted to the turbine blade at the **green imprints** on the turbine as shown in the figure. The dimension of the blade was given constraints so as to achieve accurate model.

5.3.4 Boundary conditions & loading on the turbine blade

The modeled blade was loaded onto the 'ANSYS Mechanical' tab to perform the analysis. In order to perform the composite layup, the blade was modeled as a shell element. **6mm** of PVC 60 kgm^3 Foam was added to the shell.

Boundary conditions: A fixed support was applied to the struts as it best simulated the actual conditions of the blade.

Loading: A force of 5000N was applied to the side of the blade to simulate the force exerted by the wind on the turbine. 5000N force was applied since it's the maximum aerodynamic load experienced by a vertical axis turbine blade of 1m long. Other loading conditions such as torque & vibration were not considered since the wind speed in the **Mesa area** was less in order to cause any of the above mentioned forces.

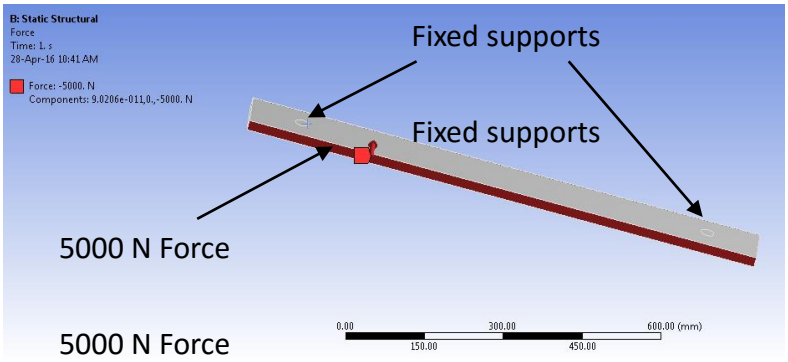

FIGURE 8: FIXED BOUNDARY CONDITION & LOADING

5.3.5 Simulation on the turbine blade

Based on the above criterion, the simulation was performed and the following results were obtained:

Maximum Stress = 95.7 MPa

Total Deformation = 194.15 mm

We can clearly see that the foam deforms severely under the aerodynamic load. The foam if used alone would fail under this load. These results were taken as parameters for the optimization process. In order to strengthen the blade, the composite layup was to be performed.

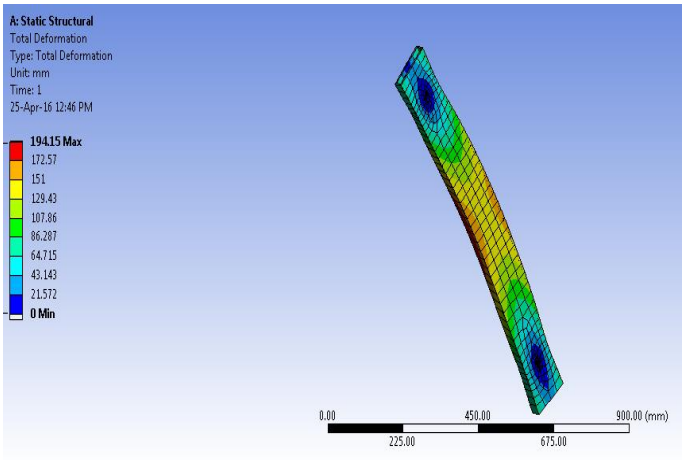

FIGURE 9: TOTAL DEFORMATION IN THE FOAM

5.3.6 Composite Layup Process

The ANSYS Composite PrePost (ACP) module was used to perform the composite layup on the turbine blade. There are various considerations that have to be taken during the layup process such as [5.9]:

- Selection of the material i.e. unidirectional or bidirectional
- Thickness of the ply
- Orientation of the ply
- Resin used to bonding the plies to form the laminate
- Positioning of the oriented plies in the laminate
- Symmetrical or unsymmetrical layup of the plies

The Concept behind the layup process that was performed in ANSYS ACP are as follows [5.8]:

- 90 degree plies were placed in the outer part of the laminate as it helps reduce the stress acting on the blade. Furthermore, it prevents the delamination of plies
- A symmetric layup of $[(90/45/-45/0)]_s$ ply layup was selected as they provided the material with isotropic properties which helped in the analysis of the material. Furthermore, this stacking or layup process provide the greatest resistance to the delamination process.
- The thickness of the fibers were taken as 1mm and the resin thickness was taken as 0.25mm

Based on the above discussions and advantages of the layup, the ANSYS ACP was made use and the layup was performed for both the carbon fiber & EGlass fiber composite material. The same layup sequence was used for both the materials which facilitated in a better comparison. The following image shows the layup of the composite.

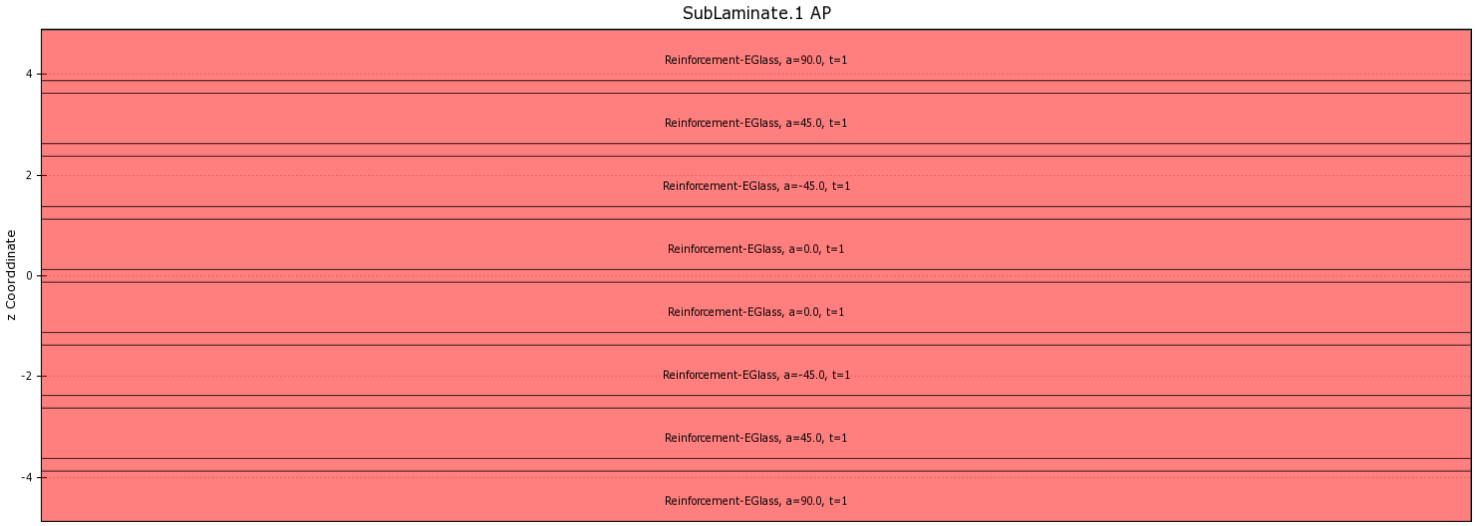

FIGURE 10: SYMMETRIC LAYUP OF THE PLIES

From this stacking/layup, we can clearly see that above mentioned symmetric layup with 90 degree plies on the outside and each composite fiber is bonded using the epoxy resin. The total thickness of the laminate was **9.75 mm**.

5.3.7 Simulation on the turbine blade after laminate layup

The static structural simulation was performed on the turbine blade after the layup process for the same loading conditions and the boundary conditions. The results obtained are as tabulated below.

TABLE 5: FEA ANALYSIS ON THE PVC FOAM

Composite	Maximum Stress (MPa)	Total Deformation (mm)
Glass reinforced plastic	69.46	0.38
Carbon filament reinforced plastic	72.72	0.19

The results show that just by adding 9.75 mm of the composite laminate, the stress and the deformation reduced to a great extent. Both the composite materials provided remarkable structural properties to the turbine blade and made use of a mere 9.75 mm of material to achieve this. However, we can see that the stress is still higher than the maximum stress of the PVC foam. Also, the optimal thickness of the plies based on the mathematical model is to be determined.

In order to reduce the stress acting on the turbine blade and also to optimize the thickness of the plies, the optimization study was performed. Furthermore, based on the optimization study the best material is to be selected.

5.4 Optimization Study

5.4.1 Design of Experiments

Based on the results obtained after the simulation of the composite material, the next step was to perform the optimization study on the thickness of the material. The 'Design of Experiment' module of the ANSYS Workbench was used to perform the optimization study.

As discussed in section **5.2.5.2**, the seven parameters were considered for the optimization study. These parameters were formed in the ANSYS Parameter set. The parameters were as follows:

- Input Parameters
  - Epoxy thickness
  - Fiber thickness
  - Foam thickness
- Output Parameters
  - Laminate thickness
  - Maximum stress
  - Total deformation

Once the parameters were defined, the bounds of the parameters were defined in the design of experiments module. The bounds of each parameter are as follows.

TABLE 6: UPPER AND LOWER BOUNDS OF THE PARAMETERS

Parameter	Initial Value	Upper Bound	Lower Bound
Minimize laminate thickness	9.75 mm	-	-
Epoxy thickness	0.25 mm	0.5 mm	0.75 mm
Fiber thickness	1 mm	1.5 mm	0.5 mm
Foam thickness	6 mm	7 mm	5 mm

The design of experiments was setup to perform the optimization. The following type of design of experiment was made use [5.10]:

- Latin Hypercube Sampling (LHS) was used to perform the DOE analysis. LHS is a unique sampling technique as it helps in generating a sample of logical collections of the parameter values. As the name says, a cube set of equal number of rows and columns are formed which contain the parameter values
- A user-defined sampling size of 100 sample/design points was used to run the DOE analysis. By doing so, the parameter values were divided into 100 logical values based on the upper & lower bounds of each parameter

The ACP module was used to analyze each of the 100 design points and the values of deformation & maximum stress was tabulated. Based on these results, the surface response and the optimization was carried out.

5.4.2 Surface Response Analysis

Response surface analysis is technique involving the mathematical & statistical data to determine the change in the output variables when the input variable is changed [5.11]. When a suitable design of experiments is setup, the response of the variables can be easily determined. The response surface is constructed in an iterative manner. Based on the design of experiment samples, the response surface of the variables are computed.

A goodness – of – fit is determined from the response surface analysis that basically tells us whether the solution determined is satisfactory. If there are lots of errors in the simulation, the response surface analysis is restarted until a better result is determined.

Furthermore, a sensitivity analysis is performed during the response surface analysis which shows which parameters affect the system to a greater extent.

There are several algorithms used to perform the response surface analysis such as the Full 2nd order polynomial, neural network and kriging. For this analysis, the kriging algorithm was made use for the following reasons [5.12].

- Kriging is an optimal interpolation method based on the regression against the DOE design points and the variance observed in the solutions. A weighted sum of data values is used for the interpolation process which ensures that a fairly good estimate of the values are obtained
- Kriging helps in the estimation of the error along with the estimation of the variable

The response surface module was used to perform the above mentioned analysis. The goodness – of – fit, response of the variables and the sensitivity analysis of variables were determined form the analysis.

5.4.2.1 Goodness – of – fit

The fit of the DOE results were plotted for both the composite materials. A good understanding of the parameters was obtained from the goodness – of – fit results. It was observed that the error of

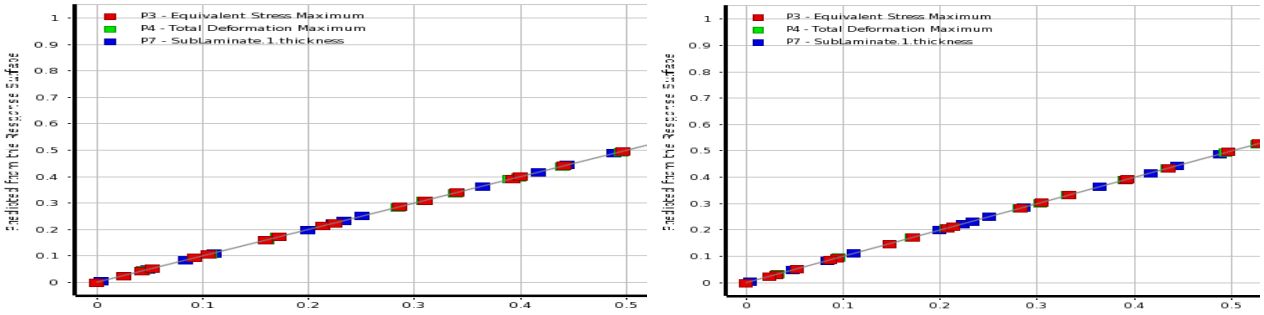

FIGURE 11: GOODNESS – OF – FIT OF OUTPUT PARAMETERS OF CARBON COMPOSITE; DOE RESULTS VS RESPONSE SURFACE RESULTS

the values calculated by the DOE analysis to the values calculated by the response surface analysis was just **1% for the carbon composite & 2% for the EGlass composite**. This tells us that a good DOE analysis was performed with very low variance.

5.4.2.2 Response Surface Plots

Based on the results calculated in the DOE analysis, the response surface algorithm determined the variation of output variables due to the changes in the input variable. The response plots were obtained from the analysis. The following conclusions were obtained from the plots:

- The thickness of the fiber material showed a huge impact on the stress and the deformation of the turbine blade. It could also been seen that the EGlass fiber performed much better than the carbon fiber for the same thickness.
- The deformation & stress in the blade were found to be about 0.43 mm & 56 MPa with the EGlass fiber of 0.9 mm thickness. For the same thickness of the carbon fiber, the deformation & stress were found to be 0.22 mm & 71 MPa.

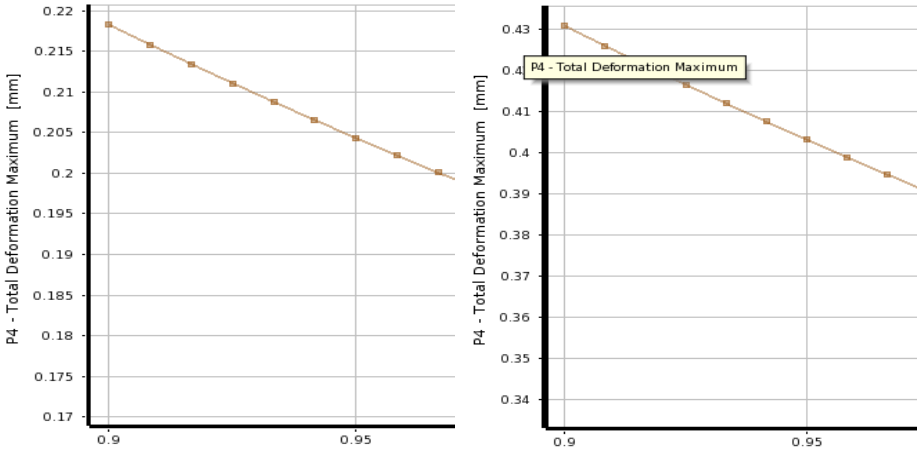

FIGURE 12: PLOTS SHOWING THE TOTAL DEFORMATION IN THE CARBON FIBER (LEFT) AND EGLASS FIBER (RIGHT)

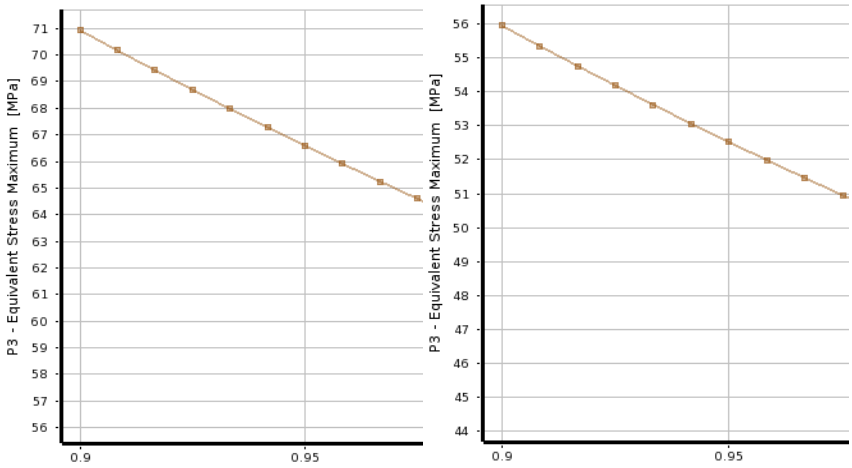

FIGURE 13: PLOTS SHOWING THE MAXIMUM STRESS IN THE CARBON FIBER (LEFT) AND EGLASS FIBER (RIGHT)

5.4.2.3 Sensitivity Analysis

The surface response analysis facilitated in knowing which input parameter affected the system to the greater extent. The results helped us understand the following:

- The equivalent stress reduced drastically with a slight increase in the fiber thickness for both the composites
- The total deformation was clearly the most affected in the system. A slight positive increase in the fiber thickness provided high structural properties with reduced deformation

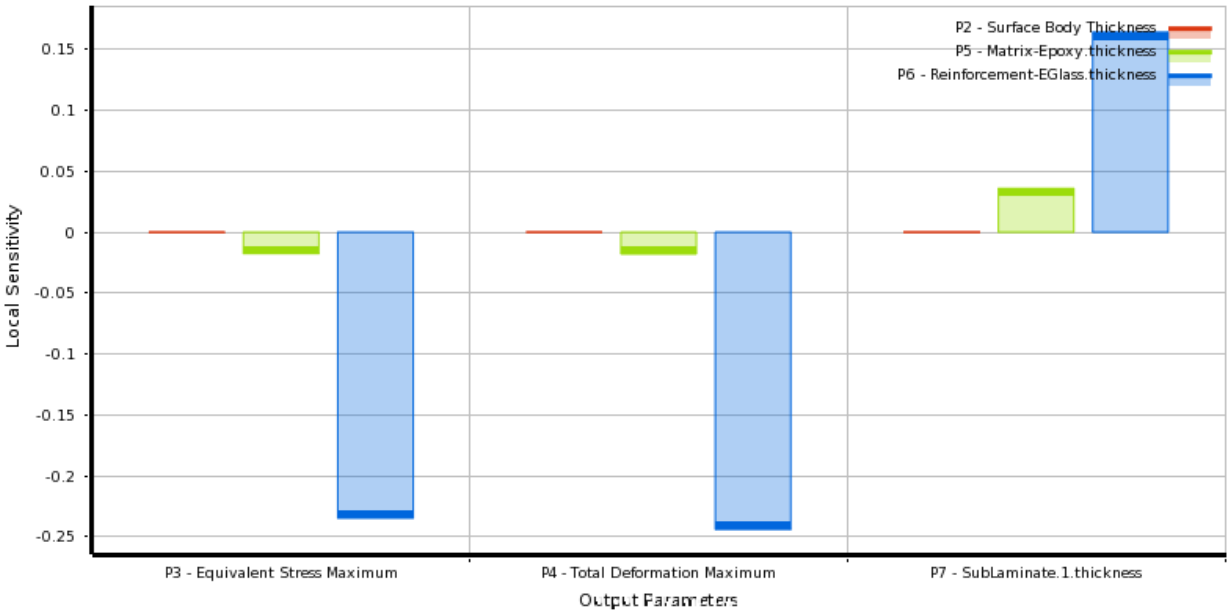

FIGURE 14: SENSITIVITY OF THE OUTPUT PARAMETERS TO CHANGES IN THE INPUT PARAMETERS FOR BOTH THE COMPOSITE MATERIALS

5.4.3 Optimization Analysis

Once the DOE & the response surface results were obtained, the input parameters were to be optimized for achieve the desired constraint values. In order to do so, the Optimization module of the ANSYS Workbench was used. As discussed in **section 5.2.6** the laminate thickness was to be minimized with PVC stress constraint of 65 MPa and the total deformation constraint of 2 mm.

ANSYS consists of several optimization algorithms such as screening, MOGA, NLPQL and MISQP that can be selected based on the objective function. The NLPQL – Non Linear Programming by Quadratic Lagrangian was selected as the optimization algorithm for the following reasons [5.13]:

- As the objective function is a continuous function of variables and constraints, the NLPQL algorithm provides the very good optimal
- Since there exists only one objective function, the NLPQL algorithm was selected

- The gradient based Lagrangian is used for the approximation of the solution with a linearization of constraints. The search direction is determined using the QP subproblem
- The BFGS algorithm is used to determine the optimal solution with suitable penalty functions to account for the constraints

The optimization algorithm was used to analyze the 100 design points determined in the DOE analysis. At the end of the optimization process, a Pareto plot was obtained which is a plot of the optimal values of the laminate thickness with the output parameters. A total of 8 feasible points for EGlass composite was obtained whereas there existed 7 feasible points for the carbon composite.

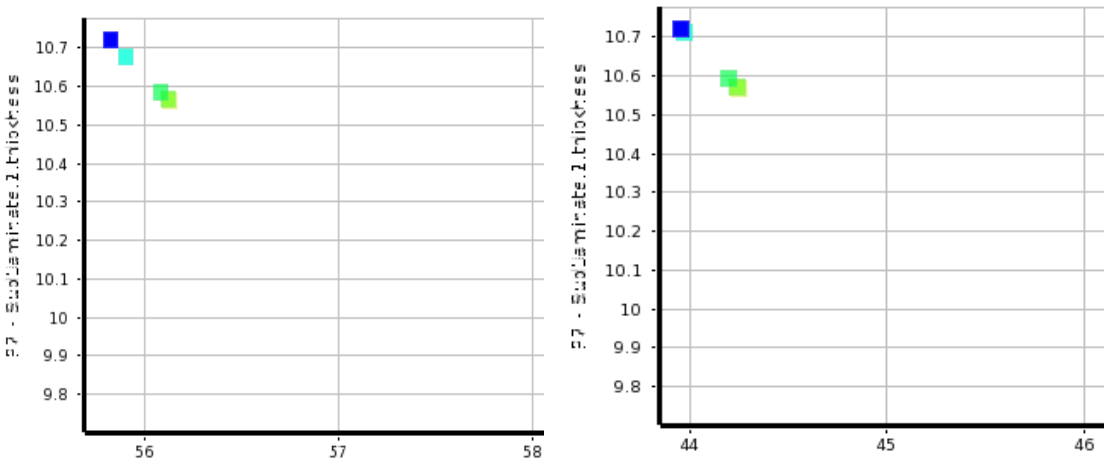

FIGURE 15: PLOTS SHOWING THE FEASIBLE POINTS OF CARBON FIBER (LEFT) AND EGLASS FIBER (RIGHT)

The optimization module selected the 3 best feasible points from the Pareto plot and was determined as the optimal solutions for both the composite materials. By analyzing the feasible points, the best optimal solution was selected for both the composites and the results are tabulated.

Initial values:

- Foam thickness = 6 mm
- Epoxy resin thickness = 0.25 mm
- Fiber thickness = 1 mm

TABLE 7: OPTIMIZATION RESULTS

Material	Foam Thickness (mm)	Epoxy Thickness (mm)	Fiber Thickness (mm)	Laminate Thickness (mm)	Equivalent Stress (MPa)	Total Deformation (mm)
Carbon-Epoxy	8.2	0.255	1.1	10.587	56.1	0.18
Eglass-Epoxy	6.5	0.275	1.1	10.596	44.1	0.33

5.5 Parametric Study

A parametric study was performed by varying the thickness of the fiber ply of the composite materials. The simulation was performed for 2 thickness i.e. 0.9 & 1.2 mm. based on the sensitivity analysis, the output parameters changed which was determined during the optimization study. This parametric study validates that the above optimization study is satisfactory and there by provides a good criterion for the material selection.

5.6 Discussion of Results

Based on the results obtained from the optimization study, we can clearly see that for the same laminate thickness of about 10.5 mm for both the materials, the EGlass composite provided a better structural property to the blade than the carbon composite. The EGlass composite offered a higher Factor of Safety for the turbine blade with almost negligible deformation. Moreover, the total blade thickness was found to be about 17 mm for the EGlass composite whereas it was 18.7 mm for the carbon composite.

We can understand from the results that the EGlass composite performs better with lesser material and there by meets the defined objective of minimizing the thickness of the laminate. As a result, the EGlass – epoxy composite material was selected as the best material for the turbine blade.

The mass of the turbine blade was determined from the optimization study for the EGlass composite material. For 10.5 mm of the composite material, the mass came up to be 17.4 kgs. An additional 3 kgs was determined for the PVC foam. A total weight of 20.4 kgs was calculated for one turbine blade.

TABLE 8: COST OF THE BLADES FOR ONE WIND TURBINE

Material	Weight (kg)	Cost ($ / kg)
EGlass – Epoxy Composite	17.4	32
PVC Foam	3	18

Cost of Material	$ 560
Cost for Layup	$ 150
Total Cost per turbine blade	$ 710
Total cost for 3 turbine blades	$ 2130

We can see that the cost of the blades for each turbine comes up to be $2130. In the system integration, the cost of the blades for the wind farm will be computed.

6. AERODYNAMIC BLADE DESIGN AND SIZE SUBSYSTEM – MATTHEW BRAUSCH

The blades of wind turbines serve as the driving component of the system. The natural flow of air over the turbine blades generates positive force due to variance in pressures around the body of each blade. For a vertical axis wind turbine, each blade makes a full rotation implying the blade undergoes a change in the angle of the blade to the free stream air from 0° to 360°. Because of this unique constraint on vertical axis turbines, the blade profile must be adequate under a large range of angles of attack. The average coefficient of lift over a full rotation of the blade should be maximized while the average coefficient of drag should be minimized. In addition to airfoil profile, the size of the blade is critical. Because the blades are mounted a fixed radius from the central hub, large moments are induced on the struts and the connection to the hub. To successfully optimize the vertical axis wind turbine, the volume, which is directly proportional to the weight, should be minimized while the tangential force produced from the blades should be maximized.

The objective of the aerodynamics subsystem is to identify the shape and profile of the turbine blades which produce the highest coefficient of performance while maintaining feasible dimensions.

6.1 Nomenclature

Nomenclature for aerodynamics subsystem

C_D	=	Coefficient of drag
C_L	=	Coefficient of lift
C_T	=	Tangential force coefficient
Θ	=	Azimuthal angle (degrees)
α	=	Relative angle of attack (degrees)
λ	=	Tip speed ratio
c	=	Blade cord (m)
h	=	Blade length (m)
A_{plan}	=	Planform area of a single turbine (m^2)
A_{swept}	=	Swept area of the VAWT (m^2)
R	=	Radius of the VAWT (m)
AR	=	Aspect ratio
N	=	Number of turbine blades
σ	=	Solidity
v_∞	=	Free-stream wind velocity (m/s)
ω	=	Rotational velocity (rad/s)
W	=	Relative velocity of a turbine blade (m/s)
V	=	Volume of a single turbine blade (m^3)
V_{max}	=	Maximum allowable volume of a single turbine blade (m^3)
$F_{T\,avg}$	=	Average tangential force of a single turbine blade per full rotation (N)
COP	=	Coefficient of performance
ρ_{air}	=	Density of air (kg/m^3)

The designated variables for the optimization process are c, h, λ, and AR. These parameters change throughout the optimization process and are used to calculate the remaining characteristics of the wind turbine once the optimization is complete.

6.2 Mathematical Model

The mathematical model for the aerodynamics of the subsystem was derived from the basic equation for the coefficient of performance for a wind turbine. The constraints and assumptions which influenced the objective function are contained in detail in the following sections.

6.2.1 Turbine Blade Profile Selection

Prior to formulating the objective the type of basic profile of the airfoil needed to be identified before developing the problem further.

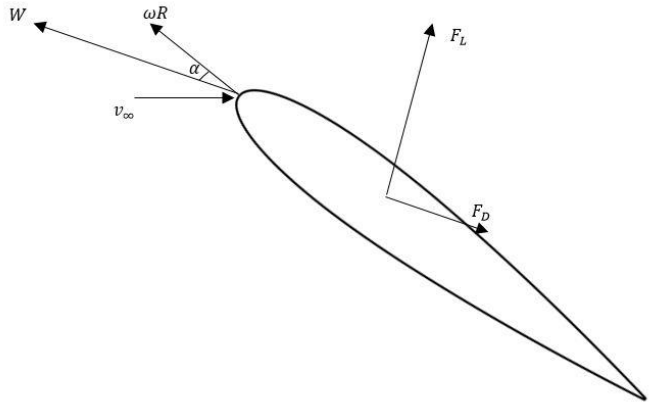

FIGURE 16: FORCE DIAGRAM OF THE TURBINE BLADE

For vertical axis wind turbines the rotation of the blade along a circular path has two major implications on the selection of the profiles. The first implication is the need for adequate performance across a large array of angles of attack. As the wind turbine rotates, each turbine blade rotates through a cycle of orientations to the free-stream velocity. This orientation to the free-stream velocity is denoted as Θ, or the azimuthal angle. While the free-stream velocity acts at the orientation Θ the actual angle of attack is a factor of the azimuthal angle, the rotational velocity, and free-stream velocity. This relationship is shown in the Eq. 6.1 provides the method for the calculation of the angle of attack. [6.1]

[6.1]

$$\alpha = \tan^{-1}\left(\frac{\sin\Theta}{\lambda + \cos\Theta}\right)$$

In the calculation of the angle of attack, the tip speed ratio is a function of the rotational velocity and the free-stream velocity given in Eq. 6.2.

$$\lambda = \frac{\omega R}{v_\infty} \quad [6.2]$$

At a tip speed ratio of 1, the range of angles of attack of the airfoil would be from -60° to 60° over a full rotation of the wind turbine. Unlike typical horizontal axis wind turbines with a fixed angle of attack, the variation requires special attention to the attitude of the profile across the entire range.

The second implication of the rotational motion of the vertical axis wind turbines is the induced camber on the blade. Due to the curvilinear motion, pressure profiles along both faces experience regional fluctuations which mimic the result of camber on an airfoil profile. [6.2] With the attitude of camber, the introduction of physical camber to the airfoil profile generates undesirable pressure distributions along the inward surface of the profile.

Because of these two implications of the rotational motion, the final airfoils needed to be symmetric to provide favorable lift and drag coefficients without the negative effects of camber. To meet these needs, five symmetric NACA 4-series airfoil profiles were selected. Data for the NACA 0012, NACA 0015, NACA 0018, NACA 0021, and NACA 0025 were obtained from Sandia National Laboratories for use in this optimization project.

6.2.2 Average Force Function

The primary objective of the aerodynamic subsystem is to select the turbine characteristics which extract the greatest amount of energy from the free-stream velocity. The energy produced by the wind turbine is directly related to the tangential aerodynamic force generated by the turbine blades. Because the blades experience continuously changing forces, it is useful to develop an average force equation to represent the average force on the blade for an entire rotation. [6.3]

$$F_{T_{avg}} = \left(\frac{1}{2}\right) \rho_{air}\, c\, h \int_0^{360^\circ} C_T(\Theta)\, W(\Theta)^2\, d\Theta \quad [6.4]$$

For the average force on a single turbine blade for one rotation, the tangential force coefficient and relative velocity at each feasible instance around the rotation must be approximated. The tangential coefficient of force arrives from the tangential components of the lift and drag on the airfoil. Therefore the average coefficient of tangential force can be approximated by finding the mean for one rotation shown in Eq. 6.4 and Eq. 6.5. [6.3]

[6.5]

$$C_T = C_L \sin\alpha - C_D \cos\alpha$$

$$C_T = \left(\frac{1}{n+1}\right)\sum_{i=1}^{n} C_{L_i} \sin\alpha_i - C_{D_i} \cos\alpha_i$$

In Eq. 6.4 and Eq. 6.5 the angle of attack is a function of the azimuthal angle and the tip speed ratio shown in Eq. 6.1. For this problem, the value of n is set to 73 (360/5) so the averaging is done with tangential force samples at 5° intervals. It should also be noted, the data for the lift and drag coefficients for the specified airfoils was used to develop 6th order polynomials for the approximation of the coefficient of lift and the coefficient of drag at specific angles of attack. These 6th order polynomials were generated using *polyfit* in MATLAB.

The same technique is used in formulating the average function for the relative velocity of the turbine blades. The average relative velocity function is taken at 5° intervals of the azimuthal angle.

$$W^2 = \left(\frac{1}{n+1}\right)\sum_{i=1}^{n}\left(v_\infty(1+\lambda\cos\Theta_i)\right)^2 + (v_\infty\,\lambda\sin\Theta_i)^2 \qquad [6.6]$$

The resulting force function for the average tangential force for a single blade for one full rotation is then given in Eq. 6.7. [6.7]

$$F_{T\,avg} = \left(\frac{1}{2}\right)\rho_{air}\; c\; h\left(\left(\frac{1}{n+1}\right)\sum_{i=1}^{n} C_{L_i}\sin\alpha_i - C_{D_i}\cos\alpha_i\right)\left(\left(\frac{1}{n+1}\right)\sum_{i=1}^{n}\left(v_\infty(1+\lambda\cos\Theta_i)\right)^2 + (v_\infty\,\lambda\sin\Theta_i)^2\right)$$

Because the tangential force function is comprised of average functions and polynomial approximations it was imperative to compare the approximation with physical experimentation. Using the same operating conditions as described in the VAWT experimentation done by Rosander, the force function approximated an average tangential force on a single turbine blade to be 36.6921N. This is a mere 0.83% difference from the load cell measurements of 37N. [6.4]

6.2.3 Objective Function

With the validity of the average force function, the objective function can be generated. The objective function accounts for the coefficient of performance of the wind turbine. The coefficient of performance is a measure of how much energy is extracted from the wind which travels through the wind turbine's swept area. This relationship is shown in Eq. 4.8 where the average tangential force function is abbreviated as $F_{T_{avg}}$. [6.3]

[6.8]

$$COP = \frac{N\ F_{T_{avg}}\ \lambda\ v_\infty}{\rho_{air}\ \left(\frac{1}{AR}\right)\ h^2\ v_\infty^3}$$

However, this relationship implies the wind turbine will generate more power as the number of blades and the force increase. Based on the understanding of the generation of force, the greatest coefficient of performance would occur at the maximum size and number of turbine blades. Thus a penalty is incorporated in the objective function based on the volume of the turbine blades compared to the maximum allowable volume of the turbine blades. For this optimization problem the volume limit for one blade is $0.25\ m^3$ for a simplified rectangular volume approximation of the turbine blade.

[6.9]

$$V_{ratio} = \frac{c^2\ h\ \left(\frac{t}{c}\right)}{V_{max}}$$

In Eq. 6.9 the maximum thickness in terms of cord length of the airfoil profile is given as $\left(\frac{t}{c}\right)$. This thickness is a characteristic of the airfoil profile. Additionally, the simplified rectangular volume approximation is used because each blade is symmetric and has a constant profile. Thus the comparison of the simplified volumes is equivalent to the actual volume ratio.

The objective function is then given by incorporating these two dimensionless ratios.

$$min\ f = COP\ (V_{ratio} - 1) \qquad [6.10]$$

6.2.4 Assumptions

In order to arrive at a developed objective function several assumptions were made to reduce the complexity of the model.

- The number of blades can range from 2 to 5 blades. This assumption is based on previous experimentation and optimization of vertical axis wind turbines. The number of blades is not included as a variable in the optimization process because it is manually changed for each optimization.
- The volume of the blade is directly proportional to the weight and therefore the cost of the turbine blade.
- The aerodynamics of the blade supports are not considered in the aerodynamic optimization of the blade itself.
- Only symmetric airfoil profiles are considered for this optimization.
- The coefficient of lift and drag data was measured at a Reynolds number of 80,000 which is assumed to be the mean operating conditions of the wind turbine.
- The height of the blade must be greater than the chord length to reject the optimization's attempt to select a chord length of infinity.
- The air speed is set to 8mph based on weather data for Mesa.
- Dynamic stall is ignored to reduce the complexity of the approximation of the tangential force component at high angles of attack.
- The effect of turbulence on the downstream turbine blades is negligible at sufficiently low wind speeds.

These assumptions allow for a more efficient optimization which still provides insight into the optimal design of the wind turbine blades for the given location.

6.2.5 Constraints

The constraints for the optimization are based on previous studies of vertical axis wind turbines as well as regulations placed on turbine sizing in residential locations. Additional constraints are implied based on the defined set of constraints but are not included to avoid redundancy on the constraints of the system.

- The chord length of the airfoil must be non-negative but less than the height of the blade.

- The height of the turbine blade must greater than the chord length but less than 5m. 5m presents the upper limit for vertical axis turbines before they become exceedingly large for small scale, urban implementation. [6.4]
- Tip speed ratio should be greater than 0.1 but less than 8. Typical Darrieus straight blade VAWTs possess a cut-in (starting point of power generation) at a tip speed ratio of 4; however, the simulation conditions due not accommodate the possibility of large tip speed ratios so the lower bound remains below the cut-in point. [6.5] [6.6]
- The aspect ratio of the turbine should be greater than 0.1 but less than 2. As the aspect ratio increases the maximum allowable efficiency of the VAWT decreases considerably. [6.7]

$$AR = \frac{h}{R} \qquad [6.11]$$

The constraints on the aspect ratio in turn place constraints on the radius of the system according to the optimized height.

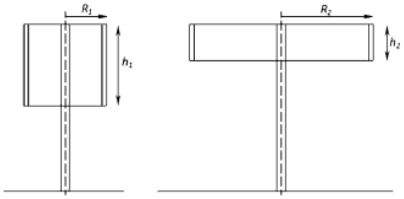

FIGURE 17: BLADE PROFILE

Figure 6.2.5.1 High aspect ratio (right) vs. low aspect ratio (left)

- The solidity of the vertical axis wind turbine should be less than 2.

$$\sigma = \frac{N\,c}{2\left(\frac{1}{AR}\right)h} \qquad [6.12]$$

Optimization studies for VAWTs typically limit the solidity to 2 with the optimal range for Darrieus straight blade turbines closer to 0.5. [6.3]

- The rotational velocity of the wind turbine should fall between 0 and 20 rad/sec. Unlike horizontal axis turbines, lower rotational speeds are necessary to avoid aerodynamic wear on the blades and the struts. [6.8]

[6.13]

$$\omega = \frac{\lambda\, v_\infty}{\left(\frac{1}{AR}\right) h}$$

- The planform area of the blades should be less than $1m^2$ for urban vertical axis turbines.
- The radius of the VAWT should be greater than 0 but less than 2.5m. This accommodates for a 5m across turbine which is rather large in the context of installation on ASU's Mesa campus.

$$R = \left(\frac{1}{AR}\right) h \qquad [6.14]$$

- The volume of a single turbine blade should be less than the maximum allowable volume of $0.25m^3$.

Some constraints on the system are implied based on the definition of the variable. For instance, the coefficient of performance is limited to be greater than 0 but less than 1. For Darrieus straight blade VAWTs the maximum coefficient of performance has be measured to be closer to 0.45. [6.7] Additionally, the range of potential angles of attack is from -90° to 90°.

6.2.6 Summary Model

The complete mathematical model for the optimization of the aerodynamics of the wind turbine blades is as follows with the objective function and the constraints.

Minimize

$$f = \frac{N\, F_{T_{avg}}\, \lambda\, v_\infty}{\rho_{air}\, \left(\frac{1}{AR}\right)\, h^2\, v_\infty^3} \left(\frac{c^2\, h\, \left(\frac{t}{c}\right)}{V_{max}} - 1 \right) \qquad [6.15]$$

Subject to

$$g_{1_1} = -V \leq 0$$
$$g_{1_2} = V - 0.25 \leq 0$$
$$g_{2_1} = -V_{ratio} \leq 0$$
$$g_{2_2} = V_{ratio} - 1 \leq 0$$

Variable Constraints

$$g_3 = -c \leq 0$$
$$g_4 = h - 5 \leq 0$$
$$g_5 = c - h \leq 0$$

$$g_{6_1} = 0.1 - \lambda \leq 0$$

$$g_{6_2} = \lambda - 8 \leq 0$$

$$g_{7_1} = 0.1 - AR \leq 0$$

$$g_{7_2} = AR - 2 \leq 0$$

Nonlinear constraints

$$g_{8_1} = -\sigma \leq 0$$

$$g_{8_2} = \sigma - 2 \leq 0$$

$$g_{9_1} = -\omega \leq 0$$

$$g_{9_2} = \omega - 20 \leq 0$$

$$g_{10_1} = -A_{plan} \leq 0$$

$$g_{10_2} = A_{plan} - 1 \leq 0$$

$$g_{11_1} = -R \leq 0$$

$$g_{ll_2} = R - 2.5 \leq 0$$

These 19 constraints serve as the bounds for the optimization of the wind turbine blades. Reaching an optimal solution within or on these bounds will provide a feasible solution to the aerodynamic subsystem.

6.3 Model Analysis

The major simplification for the problem arises in the force function. Rather than deal with a differential in the objective function, the tangential force is dealt with as an average over the range of azimuthal angles.

In terms of the constraints, the complexity of the objective limits the simplification of the constraints. Coupling of the constraints for aspect ratio, tip speed ratio, and the dimensions of the turbine blades restrict the removal of constraints without likewise influencing the other constraints on the system.

6.3.1 Monotonicity Analysis

The monotonicity analysis of the objective functions provides a tool to discuss the state of the mathematical model. For the objective functions the 4 variables should be well-constrained to ensure the objective function is well-constrained. The monotonicity analysis is shown in Table 9.

TABLE 9: MONOTONICITY ANALYSIS OF OBJECTIVE FUNCTION

Constraint	c	h	λ	AR
f	+	+	-	-
g_3	-			
g_4		+		
g_5	+	-		
g_{61}			-	
g_{62}			+	
g_{71}				-
g_{72}				+

Through the monotonicity analysis, the objective function is observed to be well-constrained. Each variable of the constrained above and below by at least 1 constraint. Thus the system is well-constrained according the Monotonicity Principle 1. Additionally, the objective function is monotonic in terms of each variable which is beneficial to the constraining of the mathematical model.

Overall, the monotonicity analysis confirms the objective function is well-constrained and will produce a solution in the feasible domain.

6.4 Optimization Study

The optimization study presents the findings of the minimization of the objective function along with the function input and initial conditions. Section 6.4.1 and 6.4.2 show the initial conditions along with the optimal solution as determined by the objective function.

6.4.1 Initial Conditions

The initial conditions for the optimization were determined based on the feasible range of solutions to ensure the objective function did not reach a point at which returned *NaN*. For example the value of tip speed ratio cannot be equal to 1 because it produces a zero in the denominator of the angle of attack calculation at an azimuthal angle of 180°.

TABLE 10: INITIAL CONDITIONS

$$c_0 = 0.5\ m$$

$$h_0 = 1.5\ m$$

$$\lambda_0 = 1.5$$

$$AR_0 = 0.5$$

$$R_0 = 3$$

$$v_\infty = 3.58\frac{m}{s}$$

$$\omega_0 = 1.79\frac{rad}{s}$$

$$\sigma_0 = 0.0833\ N$$

$$A_{plan_0} = 0.75\ m^2$$

$$V_0 = 0.375\left(\frac{t}{c}\right)\ m^3$$

Thus the initial input for the optimization function is [0.5, 1.5, 1.5, 0.5].

6.4.2 Optimal Solution

For the optimization of the turbine blade profile the initial conditions remained constant for each optimization cycle. The objective function was used to calculate to optimum airfoil profile for each NACA 4-series profile at 2, 3, 4, or 5 blades. The results of the optimization are as follows in Table 11. *fmincon* with interior point algorithm was used for the optimization of the objective function

TABLE 11: OPTIMAL SOLUTION FOR EACH PROFILE

Profile	Number of Blades	Chord Length (m)	Height (m)	TSR	AR
NACA 0012	3	0.360	1.755	0.701	1.026
NACA 0015	5	0.335	1.846	0.576	1.042
NACA 0018	5	0.343	1.782	0.599	0.983
NACA 0021	5	0.370	1.729	0.570	0.990
NACA 0025	4	0.428	1.595	0.632	0.933

The optimal design for the 5 airfoil profile present varying dimensions for the turbine based on the coefficient of performance and the volume ratio. At each of these optimal locations the optimized dimensions fall within the bounds for the four variables of the optimization. Because the optimization is not experiencing interaction with the bounds then the solution with the greatest power generation becomes the optimum. For this optimization, the NACA 0025 airfoil profile with four blades produces the highest coefficient of performance at 0.169, or 16.9% efficiency.

TABLE 12: OPTIMAL SOLUTION CHARACTERISTICS

c^*	=	$0.428\ m$
h^*	=	$1.595\ m$
λ^*	=	0.632
AR^*	=	0.933
R^*	=	$1.710\ m$
v_∞	=	$3.58\frac{m}{s}$
ω^*	=	$1.32\frac{rad}{s}$
σ^*	=	0.5
A^*_{plan}	=	$0.683\ m^2$
V^*	=	$0.073\ m^3$
COP^*	=	0.169

From the optimization the final selected solution is an interior local minimum of the objective function. Analysis of the boundary conditions shows none of the boundaries are active at the local optimum. While the formulation of the coefficient of performance might expect the maximum area for improved efficiency, the coupling of each variable restricts the optimization.

For different starting values, maximum remains relatively unchanged for the NACA 0025 airfoil profile with 4 turbine blades. The largest fluctuation in the optimal solution arises in the height of the turbine which has a range from 1.592 to 1.596. The optimal solution for various starting points are shown in Table 13.

TABLE 13: OPTIMAL SOLUTION AT VARIOUS INITIAL POINTS

Initial values	Optimal Solution	Objective Function
[0.5, 1.5, 1.5, 0.5]	[0.428, 1.595, 0.632, 0.933]	-0.120
[1, 2, 2, 1]	[0.428, 1.592, 0.635, 0.932]	-0.119
[2, 2, 2, 2]	[0.428, 1.595, 0.633, 0.933]	-0.120
[1, 5, 5, 1]	[0.428, 1.596, 0.633, 0.933]	-0.119

Based on the optimal solutions obtained through the mathematical model, the objective shows a dependence on the chord length. In each case, the minimization occurs at a chord length of 0.428m. This value remains constant while the blade height, tip speed ratio, and aspect ratio fluctuate depending on the starting point of the optimization. This assumption is confirmed in the plot of the objective function versus the chord length at the optimal solution of the tip speed ratio, aspect ratio and blade height, shown in Figure 17.

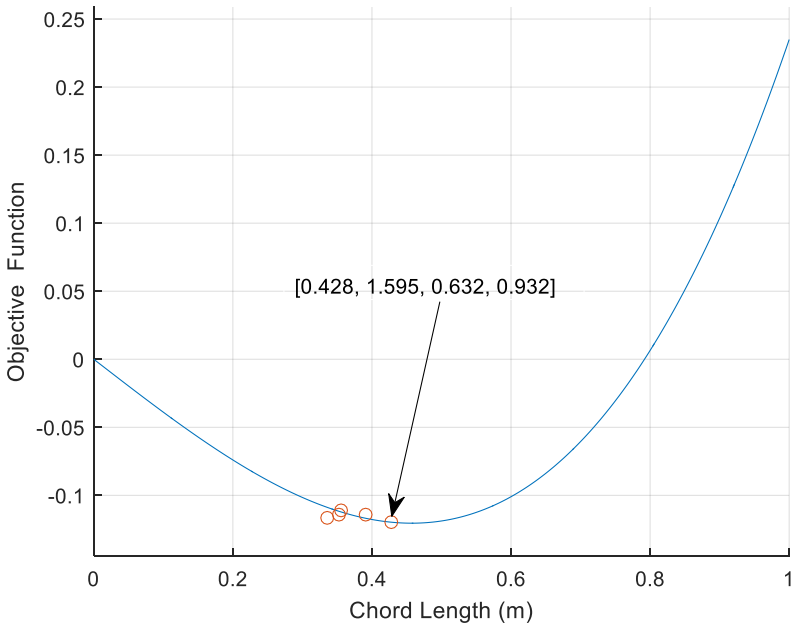

FIGURE 18: OBJECTIVE FUNCTION VS CHORD LENGTH

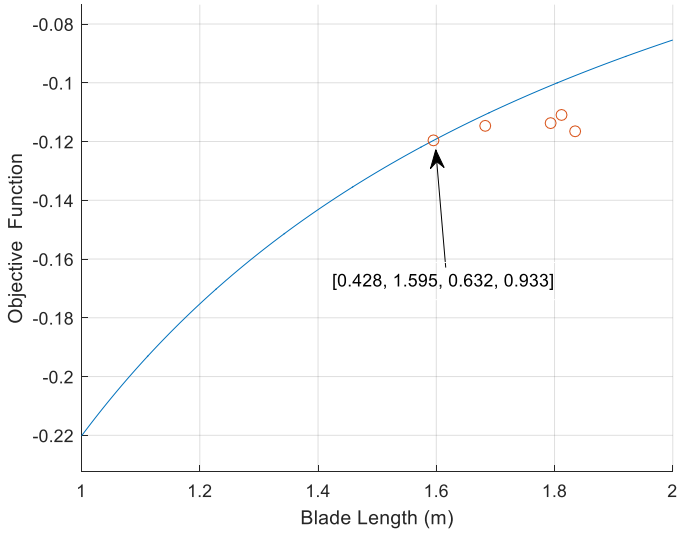

FIGURE 19: OBJECTIVE FUNCTION VS BLADE LENGTH

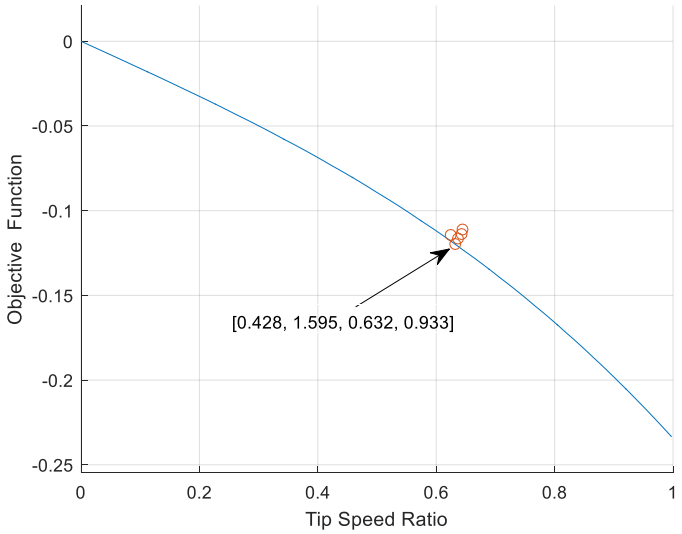

FIGURE 20: OBJECTIVE FUNCTION VS TIP SPEED RATIO

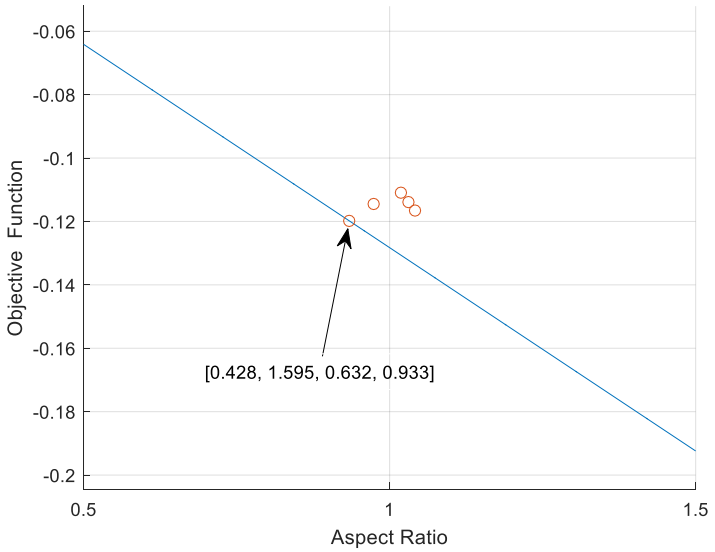

FIGURE 21: OBJECTIVE FUNCTION VS ASPECT RATIO

In Figures 18, 19 & 20, the objective function is varied based on the blade height, tip speed ratio, and aspect ratio, respectively. In each case, the optimal solutions fall along the objective function line but not at a local minimum or maximum. In contrast the objective function reaches a clear minimum at the optimal chord length, shown in Figure 17. Because of this occurrence, the optimal solution is heavily tied to the chord length. From a practical standpoint, this assumption is accurate because the volume is a function of the chord length squared so the optimum solution should occur at the maximum of the quadratic volume ratio in terms of the chord length.

6.5 Parametric Study

For the optimization of the vertical axis wind turbine for use on ASU's Mesa campus the fixed parameter is the free stream velocity, which is defined as the average velocity in Mesa. For this project, the average wind velocity is set to 8mph. However, this value is simply an average, and the actual wind turbine experiences a range from still (0mph) to gusts as high as 80mph during a monsoon. [6.9]

By varying the free-stream velocity the optimal solution for the anticipated operating conditions can be predicted. Figure 21 shows the coefficient of performance as the free stream velocity is increased from 0mph to 80mph.

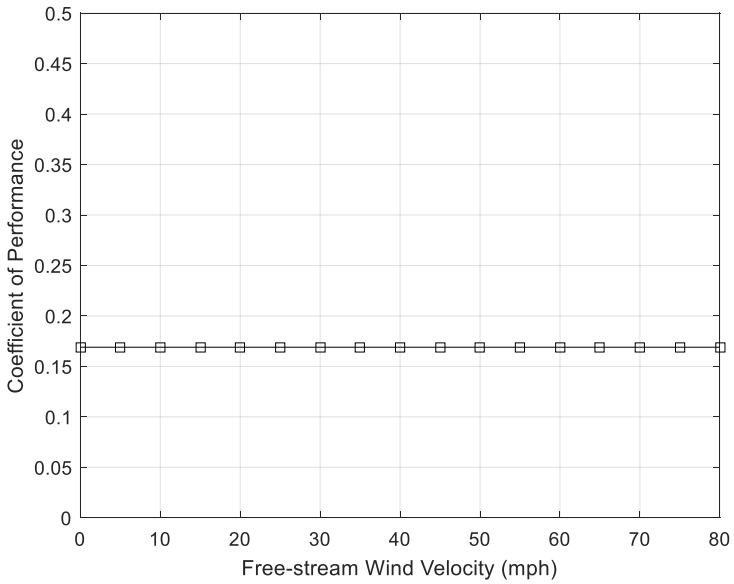

FIGURE 22: COP AS WIND VELOCITY INCREASES

The parametric study shows the free-stream velocity is not a factor on the optimal wind turbine characteristics. This result follows the prediction of the attitude of the objective function based on the free-stream velocity. In the objective function, the free-stream wind speed is cubed in the numerator and denominator (Eq. 6.15). Thus while the tangential force and power generated will increase, the coefficient of performance and the objective function will remain constant for all wind speed experienced by the turbine.

6.6 Results and Discussion

The final optimal solution for objective function presents a possible solution for creating a vertical axis wind tunnel in Mesa, Arizona. Based on the optimization study, the final design features the NACA 0025 profile and 4 turbine blades. The chord length is 0.428m and a blade height of 1.595m. This solution presents the characteristics for a vertical axis wind turbine which operates at a tip speed ratio of 0.633 and a coefficient of performance of 0.169.

From this optimization study, several design rules for the aerodynamics of vertical axis turbine blades were uncovered. The first is the lack of influence of the free-stream velocity on objective function. The parametric study of the objective function confirms this rule. The consistency of the VAWT for the full range of wind speeds is a positive attribute of vertical axis designs. Additionally, the optimization study has a heightened sensitivity to the chord length. From the early discussion, the objective function reaches a minimum which corresponds with optimal chord

length. In the case of the blade height, tip speed ratio, and aspect ratio, the objective function does not reach a maximum or minimum at the optimal solution. This is an indication of the importance of the chord length on the optimal characteristics of the wind turbine.

While this optimization presents a viable solution there are obvious drawbacks. The restrictions on the model limit the coefficient of power of the wind turbine to below 17%. The formulation of the tangential force function lacks the complexity to properly deal with dynamic stall. For vertical wind turbines especially, designing for dynamic stall dramatically increases the coefficient of performance without the need of excessively large turbine blades. [4.1] To overcome this defect of the model, future optimization can be done with Multiple Streamtube Method. The streamtube model handles the effects of dynamic stall and provides sufficiently accurate approximations for the forces on the turbine blade. [6.5]

Moving forward with the optimization, the other subsystems are not coupled with the aerodynamic properties. While the aerodynamic subsystem provides useful information for the optimization of the other components, it is still possible to optimize the support, material, and positioning without coupling the subsystem to the aerodynamic characteristics. This process can result in minor inconsistencies among subsystems but it ultimately creates a viable vertical axis wind turbine in an efficient optimization study.

7. STRUCTURAL OPTIMIZATION OF WIND TURBINE BLADE - ANKITA KARDILE

Problem Statement:

The Vertical Axis Wind Turbine (VAWT) needs to be designed for the structural integrity during its operation. Since the turbine blade is the most crucial component of the wind turbine, the structural optimization of the support structures needs to be carried out considering the extreme conditions. The different modes of blade loading are gyroscopic, centrifugal, aerodynamic, gravitational and operational loading for a VAWT. The magnitude of each of the loads will depend on the operational condition being considered. Since gyroscopic forces are the minimum among the other loads acting on the turbine blade, they are not critical and excluded from the scope of study**.** Fatigue loading on the support structure has been excluded from the scope of study to limit the computational time and complexity of the model for design optimization.

7.1 Nomenclature:

ds_cltolh	=	distance from blade centreline to top strut
ds_ctoc	=	distance from blade centreline to the bottom strut
ds_breadth	=	breadth of top strut
ds_height strut	=	height of top strut
ds_hleft	=	height of bottom
ds_bleft	=	breadth of bottom strut
ds_strutl	=	length of the struts
ds_angle, ds_angle2	=	draft angle for top and bottom struts respectively
P1	=	Total maximum deformation
P2	=	Equivalent maximum stress
P12	=	Geometric mass of the model
ds_c1dia	=	inscribed circle diameter of the triangular cuts in optimized topology integration
ds_fend	=	center to end of strut length distance in optimized topology integration
ds_extrude	=	Thickness of the strut cross section in optimized topology integration
ds_length	=	length of strut in optimized topology integration
ds_t1ctoc	=	inscribed circle center to center for triangle 1
ds_t2ctoc	=	inscribed circle center to centre for triangle 2
ds_t3ctoc	=	inscribed circle center to center for triangle 3
ds_t4ctoc	=	inscribed circle center to center for triangle 4

7.2 Mathematical Model:

7.2.1 Objective Function:

The objective function of the subsystem is to minimize the mass of the support structure for the wind turbine and maintain structural integrity of the turbine blades in order to minimize the cost of the rotor. A static analysis for the operating conditions of the wind turbine blades which will cover all loading conditions has been performed for the support structure of the VAWT. Due to the support structure experiencing low forces as compared to the HAWT, there is a huge scope for optimization of the strut design and placement along the wind turbine blade. The mathematical model of the structure requires various design variables. In order to depict the model as close to

the actual working conditions of the turbine, a large set of design variables are required. Whereas, to reduce the optimization time, the number of design variables need to be limited [7.1]. Thus the mathematical model is represented as an FEM formulation in ANSYS to be able to simulate actual working conditions and be able to optimize the problem in good time. The relation between the cost of setup and support structure is by the amount of material required by the structure.

7.2.2 Assumptions:

The material was assumed to be a composite material of Carbon Reinforced Fibre Plastic for the support structure with the following material properties:

Young's modulus in x direction: 59160 MPa

Young's Modulus in y direction: 59160 MPa

Young's Modulus in z direction: 7500 MPa

Poisson's ratio xy: 0.04

Poisson's ratio yz and xz: 0.3

Maximum wind velocity in the Tempe area was assumed to be 20 m/s which was considered for loading conditions.

7.2.3 Constraints:

The subsystem needs to be properly constrained in order to yield a feasible solution. The material for the blade is constrained by the material properties such as yield strength. A certain factor of safety needs to be considered for safe functioning of the turbine since failure of any of the blades will amount to huge losses. Depending on the profile of the VAWT (Darrieus type, Savonius type, H-type etc.) further constraints on the sizing and the projected area will have to be taken into account[7.1]. Bounds and linear constraints are imposed on the design vector during the optimization. These bounds and constraints limit the design space, such that only feasible laminate thicknesses and shapes are evaluated during the optimization. Constraints on the design variables from manufacturing and feasibility point of view have also been taken into consideration.

7.2.4 Design Variables and Parameters:

The design variables are closely related to the aerodynamic design of the blade profile. The location of spars, strut thickness and breadth and length of the struts are the design variables for the subsystem. The increase in thickness of airfoil will increase the strength of the blade, however,

it will increase the resistance/drag for the air to flow over the profile of the blade and increase the forces experienced by the support structure [7.2].

The subsystem depends on a lot of other parameters which are closely related to the structural strength of the structure such as the wind velocity, blade design and weight acting on the structure. Based on the operation of the wind turbine, the tip-speed ratio number of blades, rotor height and diameter will have an effect on the strengthening to be provided to the structure [7.1].

7.2.5 Summary Model:

The objective of the subsystem is to minimize the cost of the turbine blade construction by conducting structural analysis and optimizing the structure of the support struts for the wind turbine. The model is subject to physical constraints such as the material properties, manufacturing feasibility and total deflection. The design variables are the struts and strengthening spars used in the structure.

7.3 Finite Element Method Formulation of the Problem:

7.3.1 Geometric representation:

A mathematical model to solve the stress and deflection equations under the given loading cases is complex and difficult to develop. Thus, the solutions for the loading conditions are computed using simulations of the problem in ANSYS workbench using the APDL solver. A 3D model of the geometry of the wind turbine blade and the struts attached has been made in Solidworks as shown in figure 22. The model represents an accurate representation of the actual geometry of the blade profile. The airfoil is assumed to be NACA0018 for modelling the blade. An updated model for the overall system integration of the subsystems of the wind turbine power plant will be made after validation of results from each subsystem in order to optimize the entire system.

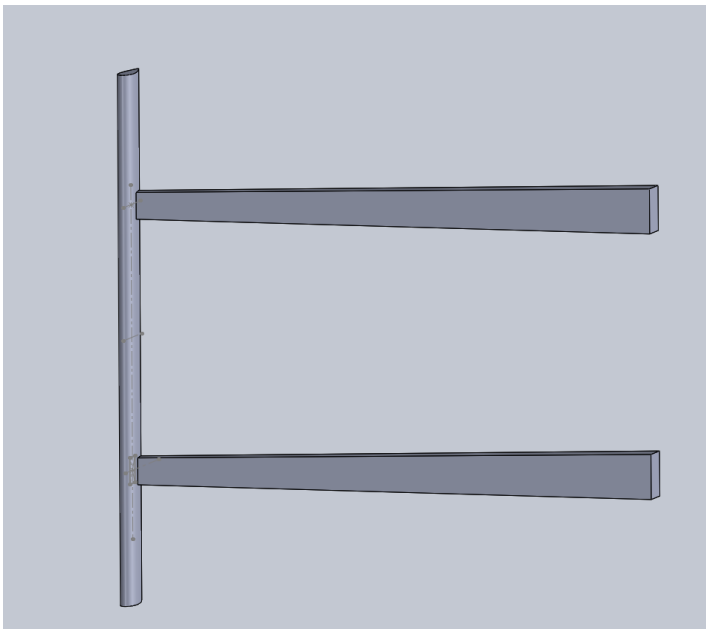

FIGURE 23: REPRESENTATION OF THE BLADE AND STRUT GEOMETRY IN SOLIDWORKS

7.3.2 Mesh generation:

The Solidworks model for the blade geometry representation was exported to ANSYS workbench to run a finite element analysis considering the loads acting on the geometry. A quadratic 3D mesh with SOLID186 elements is generated for the analysis. The quad elements form a complete and smooth mesh over the profile of the blade and hence are preferred over other types of elements. The transition at the corners of the strut to blade connection is smooth, however, this region is prone to singularities in case of fatigue loading analysis. In case of fatigue loading a width of elements around the connection shall be suppressed to allow the convergence of mesh in the analysis [7.1]. However, fatigue loading case is not considered in current scope of analysis.

7.3.3 Boundary and Loading Conditions:

The base of the struts are assumed to zero displacements on the central support of the vertical axis, whereas the connection between the blade and the struts is considered to be consistent of rigid body elements. For the current validation model, gravitational and aerodynamic loads are considered to be acting on the blade. The model was analysed and optimized for operating conditions. Since both the forces acting are body forces, equations for the force acting will be a

function of the element position from the fixed end. The applied boundary conditions and loading is as shown in figure 24.

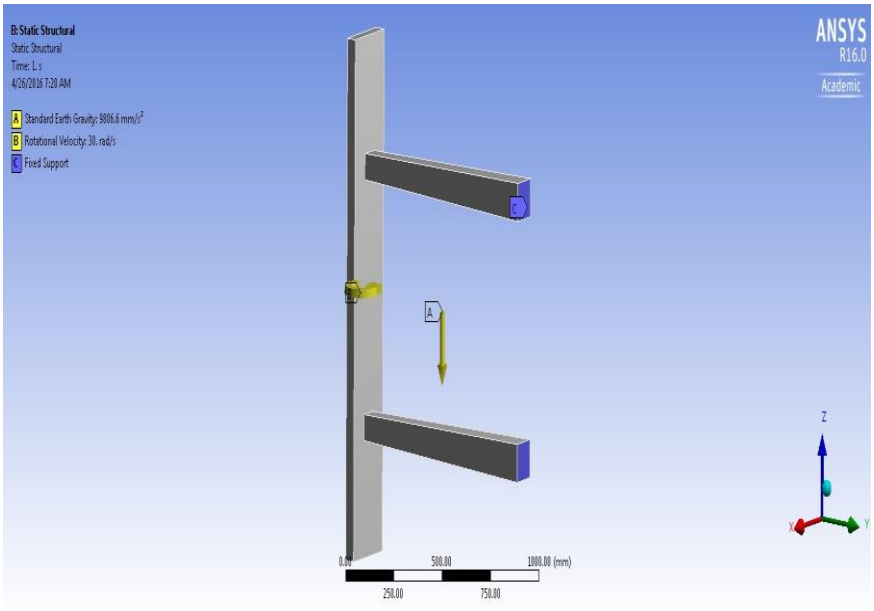

FIGURE 24: LOADING AND BOUNDARY CONDITIONS APPLIED TO THE BLADE

7.3.4 Finite Element Solution:

The result for the problem defined is shown in figures below. The maximum stress (Von-misses) and deformation obtained from the solution are parameterized in ANSYS so as to be considered as output parameters used on the Design Optimization setup.

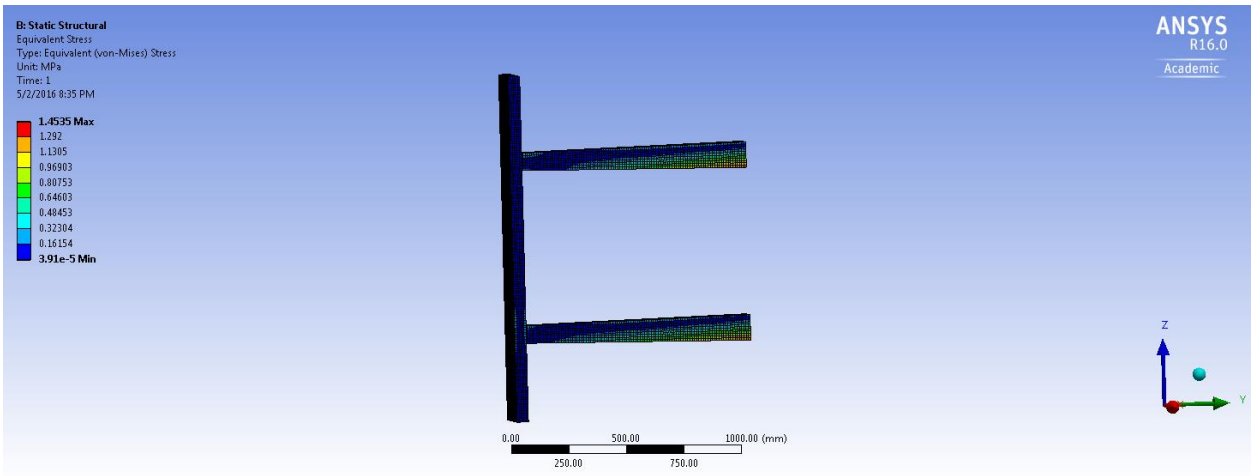

FIGURE 25: FEM RESULT FOR EQUIVALENT STRESS CONTOUR PLOT

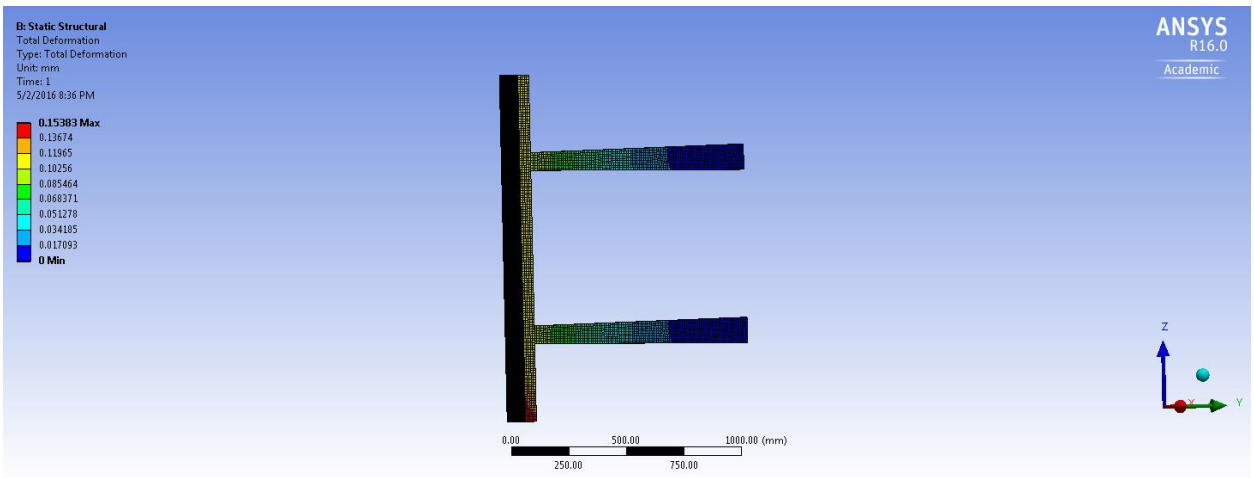

FIGURE 26: FEM RESULT FOR TOTAL DEFORMATION OF THE STRUTS

7.4 Design (Shape) Optimization:

After running the model for a finite element analysis, values of stress and total deformation in the struts were computed and parameterized. Each of the geometric and design parameters were varied within feasible limits using Design of Experiments. The limits for each variable were based on the constraints for each variable. The cross section dimensions were limited to 20mm. The free end of the struts is connected to the blade due to which it must have sufficient area of cross section for being able to be connected to the blade geometry. However, the objective function (mass of the support structure) decreases monotonically as the area of cross section decreases. The design space was generated using Latin Hypercube sampling for randomly generated DOE design points. A response surface was generated for the output parameters using the metamodeling method of

kriging. The goodness of fit for the model from the design points is shown in figure 27. The maximum error of the meta-model is 1.25%.

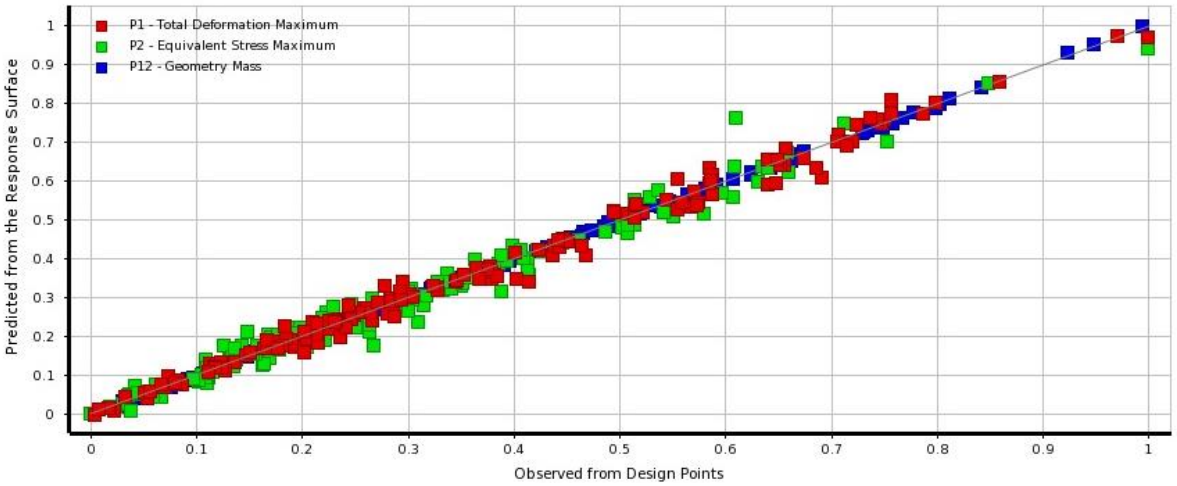

FIGURE 27: GOODNESS OF FIT FOR THE KRIGING META-MODEL FOR RESPONSE VALUES

A sensitivity analysis for each of the design variables was done so as to understand the effect of changing each of the design variables. The plot for each of the response can be seen in figure 28.

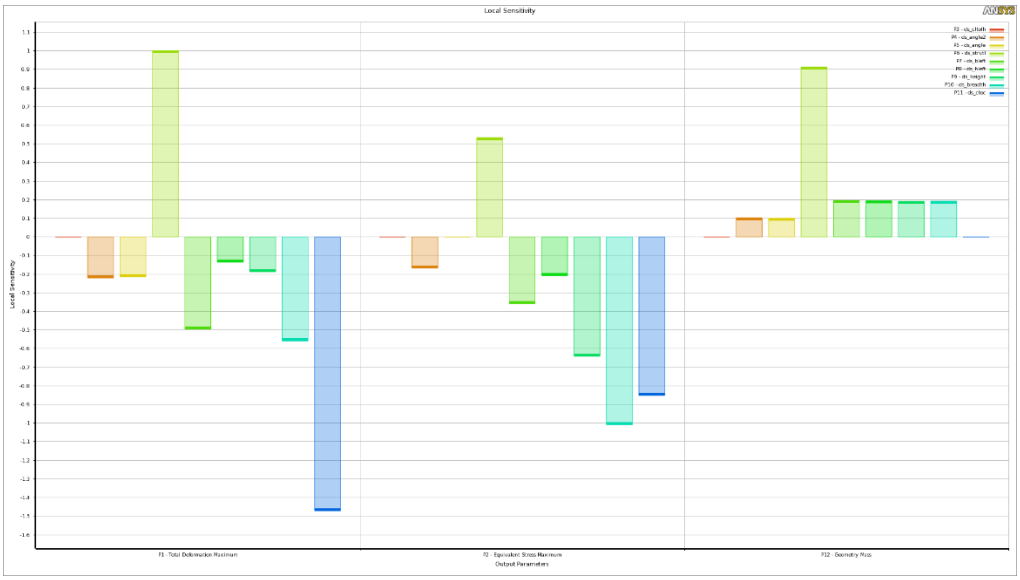

FIGURE 28: SENSITIVITY ANALYSIS FOR ALL THE DESIGN VARIABLES

Nonlinear programming by quadratic Lagrangian (NLPQL), is a gradient based algorithm suitable for local refinement of single objective with continuous parameters. It was used for the problem under consideration to arrive at the optimum solution for the mass of the struts.

7.5 Design (Topology) Optimization:

Topology optimization is a mathematical approach to optimize the material layout and distribution within the given design space. It was observed from the initial results of shape optimization that the stresses for the struts are well within limits and there is scope for further refinement of the results. An in depth study and implementation of topology optimization was carried out for the subsystem. Topology optimization for the problem was carried out using Abaqus optimization module. The problem was completely defined using the forces and supports on the respective faces of the strut. The results from the optimization study can be seen in figure 33 & 34. The 88 line MATLAB code for topology optimization written by Ole Sigmund, 2010[7.3] was modified to incorporate the loading and boundary conditions for the given problem.

7.5.1 Integration of Shape and Topology Optimization Results:

Both the results obtained from each of the optimization process were integrated by constructing a simplified representation of the optimized topology in Solidworks and parameterizing the triangular sections to be removed from the geometry. The design space was sampled for a 100 points by Latin Hypercube Sampling. The simplified version of the optimized topology is as seen in figure below.

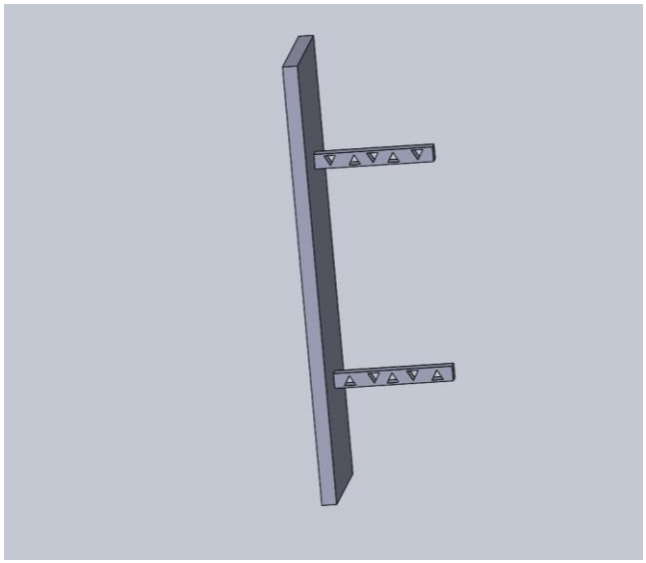

FIGURE 29: OPTIMIZED TOPOLOGY GEOMETRY INPUT MODEL

The design points were fitted by using a kriging meta-model and a sensitivity analysis was performed for the design variables of the model. The maximum error in the meta-model is found to be 0.001% indicating a very good fit of the meta-model.

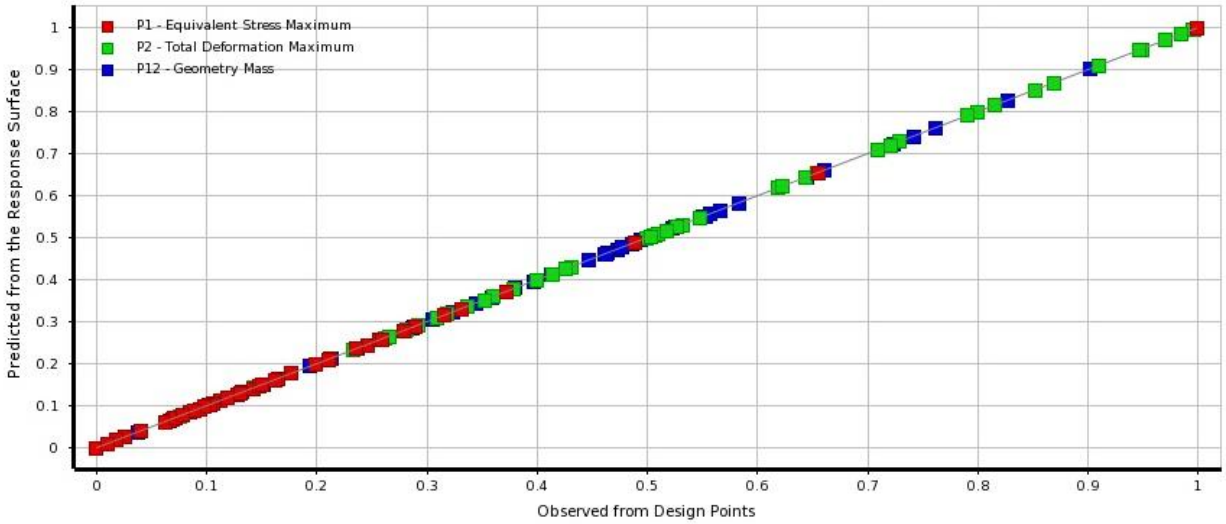

FIGURE 30: GOODNESS OF FIT FOR THE DESIGN POINTS AFTER INTEGRATION OF TOPOLOGY OPTIMIZATION RESULTS

It is observed from the sensitivity analysis as shown in figure below that none of the variables have a major impact on the geometric mass of the model. However, each of them affect the stress and deformation.

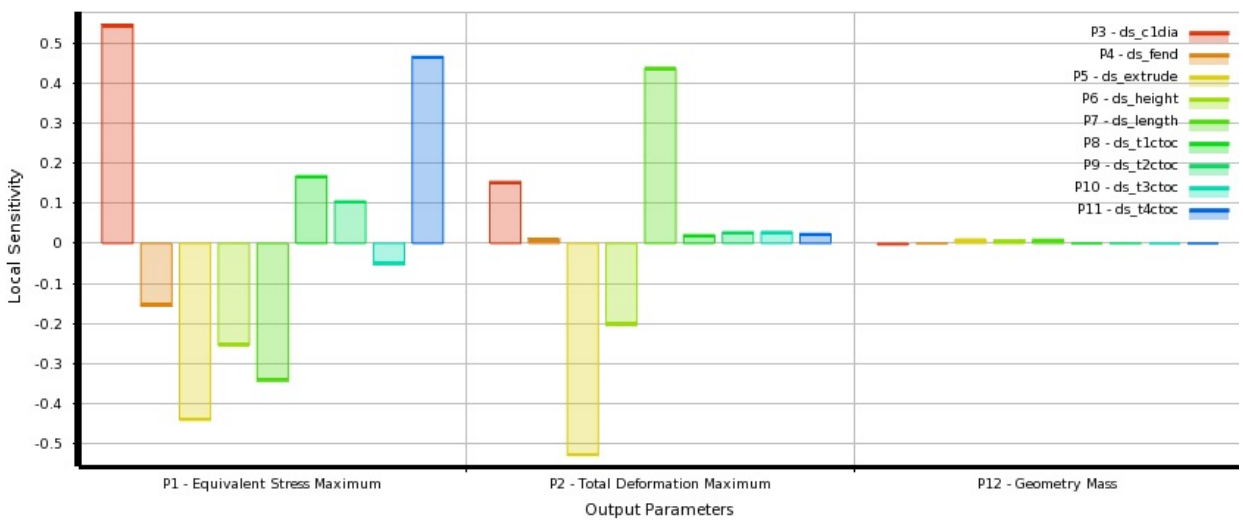

FIGURE 31: SENSITIVITY ANALYSIS FOR THE DESIGN VARIABLES AFTER INTEGRATION OF TOPOLOGY OPTIMIZATION RESULTS

7.6 Results and conclusions:

The model was evaluated for optimization over a number of design cycles by carefully varying each variable bound. It was observed that for results using screening optimization method, the resultant optimum strut dimensions were such that the top strut which experiences lower loads as compared to the bottom strut had a thinner cross-section as compared to the bottom strut. The

model was later run using NLPQL method which uses gradient based algorithm to compute the minimum. The solution converged to an optimum value in 17 iterations from the starting point. The candidate points obtained from the method can be tabulated as shown in table 14. Candidate point 2 is selected as the final optimized point since the variables are well within the feasible domain. A weight reduction of 48.26% is achieved for the total structure after the optimization.

TABLE 14: COMPARISON OF STARTING AND OPTIMUM POINT FROM SHAPE OPTIMIZATION PERFORMED IN ANSYS

Design Variable	Starting Point	Candidate Point 2
ds_cltolh	300	224.56
ds_angle2	1.2	1.6
ds_angle	1.2	1.5866
ds_strutl	1100	400
ds_bleft	62.5	25
ds_hleft	62.5	25
ds_height	62.5	25
ds_breadth	62.5	25
ds_ctoc	300	345.56
P1	0.2604	0.2433
P2	2.2858	9.7307
P12	51.179	26.477

The Pareto points for the optimization algorithm are as shown in figure below. It can be observed that since the design points are well within constraints for both stress and deformation, trade-offs for the results for better geometric mass have been taken into consideration. The points in figure 32 are all pareto optimal points because for a few points, even though the stress and deformation values are higher compared to other points, the geometric mass at these points is very low.

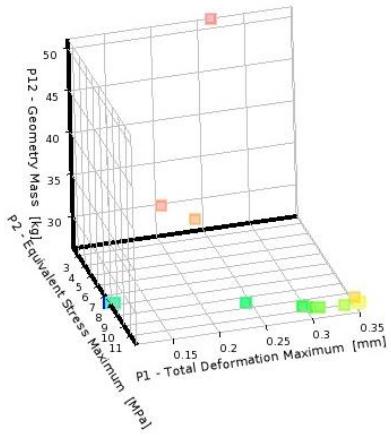

FIGURE 32: PARETO POINTS FROM THE OPTIMIZATION ALGORITHM

A major challenge in performing topology optimization was defining a well poised problem to solve. Since the loading cases on the structure consist of body forces, which depend on the mass of the geometry. As and how the material is removed, during topology optimization, from the body iteratively, the loading decreases leading to possible inaccurate results. Figure 33 shows the optimized topology from the Abaqus optimization module.

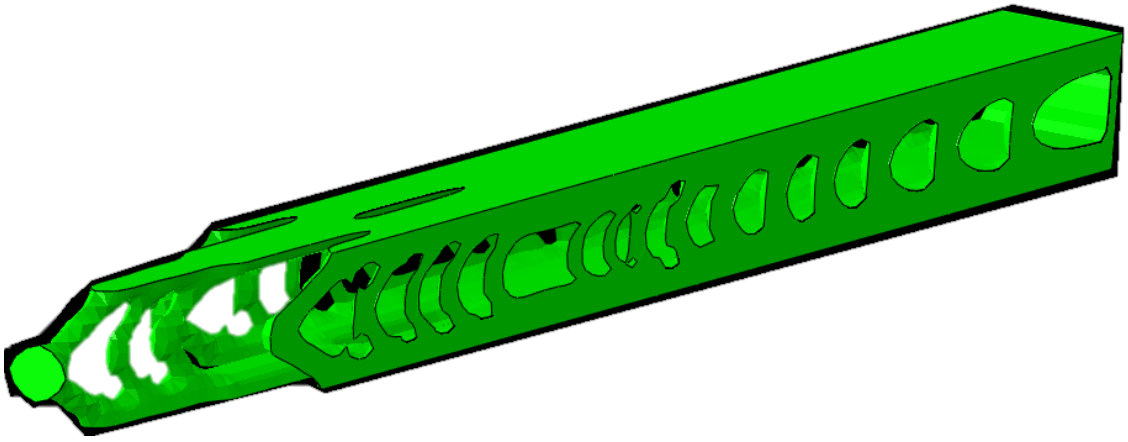

FIGURE 33: TOPOLOGY OPTIMIZATION RESULTS FROM ABAQUS OPTIMIZATION MODULE

The aspect ratio of the strut is very high (~30) due to which it is difficult to represent the entire strut in MATLAB code while specifying the number of elements in x and y direction. Hence a scaled input for both x and y elements was given in MATLAB. Abaqus output has the true dimensions. The results from both Abaqus and MATLAB are comparable with respect to the material distribution from both the methods. Abaqus as well as MATLAB make the free end remove material from the free end. Each method tries to make a truss like structure from the solid struts.

The results from Abaqus need to be refined since the material at the free end is not feasible to manufacture. Thus, the result from topology optimization was further analyzed to check the integrity of the optimized structure. The topology optimization problem was implemented using Ole Sigmund's 88 line MATLAB code by changing the forcing and boundary conditions to suit the problem of the subsystem. The optimized topology from the code is as shown in Figure 34.

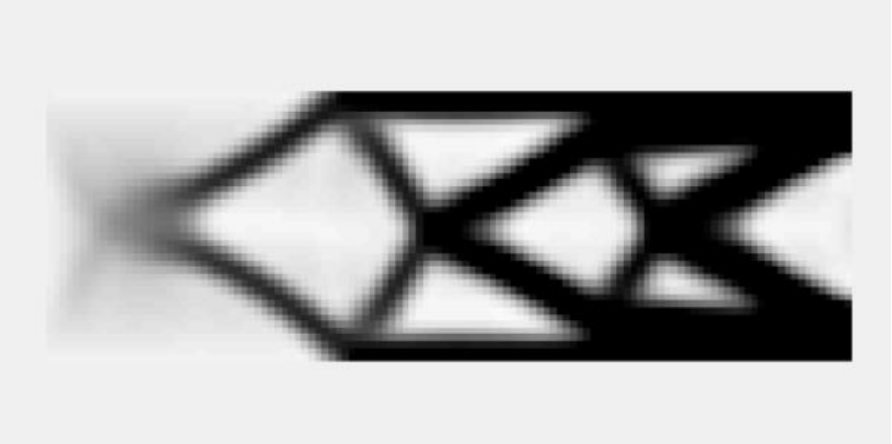

FIGURE 34: OPTIMIZED TOPOLOGY FROM 88LINE MATLAB CODE IMPLEMENTATION BY OLE SIGMUND, 2010[7.3]

As seen in Figure 33 and Figure 34, the results from both the methods are comparable. However, each of the method removes material from the free end which would not be feasible practically. Another shape optimization problem was run using the simplified optimized topology, however due to restrictions on equations relating the geometric variables of the model, a feasible optimization study is complex to be formulated. As a result of an over constrained model the percentage improvement in the weight of the strut is drastically reduced to a mere 1.8% from the initial value. The results for the optimization are tabulated as shown in 15.

TABLE 15: OPTIMUM POINT PARAMETERS FOR TOPOLOGY OPTIMIZATION

Design Variable	Starting Point	Optimum solution
ds_c1dia	22.611	24.872
ds_fend	52.414	52.943
ds_extrude	50	45
ds_length	400	360
ds_t1ctoc	86.77	91.841

ds_t2ctoc	80.92	99.74
ds_t3ctoc	67.5	71.14
ds_t4ctoc	72.725	79.179
P1	5.1474	11.517
P2	0.54303	0.81035
P12	55.754	54.753

The Pareto points for the integrated topology results can be seen in the figure below. It can be seen that the points show variation in stress and deformation along the iterations.

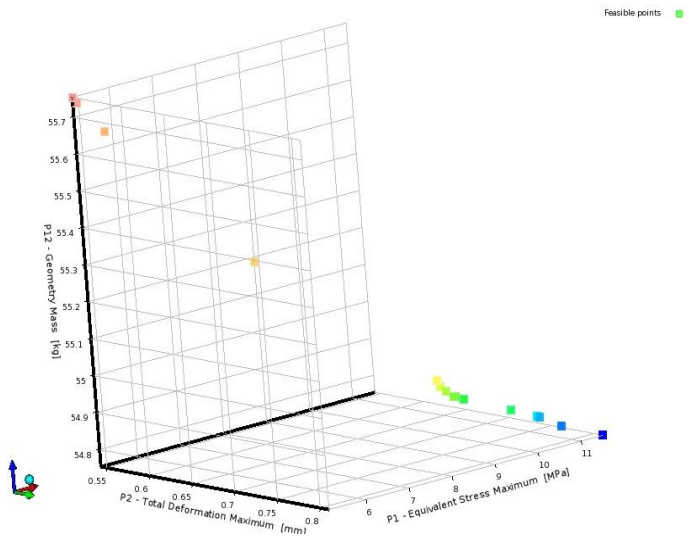

FIGURE 35: PARETO POINTS FROM THE OPTIMIZATION ALGORITHM FOR OPTIMIZED TOPOLOGY

However, the mass value remains more or less constant through the optimization process. This is due to the geometric constraints in place for the each of the design variable in order to maintain the integrity of the structure. From the results obtained from both the procedures it can be concluded that the results from the topology optimization need to be analyzed as a separate system, since the approach used in topology optimization is completely different from traditional shape optimization.

8. INTEGRATION STUDY

The objective of the entire optimization study was to create the optimal vertical axis wind turbine design to effectively operate in Mesa. The individual subsystems of the problem seek to reach this

goal through a variety of objective functions. While the optimum solutions for each subsystem provide the basis for an integrated system, it is necessary to combine the results to examine the validity of the final design.

8.1 Optimal Vertical Axis Wind Turbine Characteristics

The optimal vertical axis wind turbine for use in Mesa is a combination of the solutions from the individual optimization studies. The first component of the final design is the location and spacing of the wind turbines. Based on the optimization study the optimal number of wind turbines per square mile is 48.

The characteristics of each individual wind turbine were found using the optimization of the aerodynamic properties of the turbine blades. The final blade design was based on the NACA 0025 geometry and has a chord of 0.428m, a blade height of 1.595m, and a radius of 1.71m. The blade design results in a total blade volume of approximately $0.037m^3$ with 4 blades per turbine. This design operates at a coefficient of performance of 0.169 given the average wind speeds in Mesa.

Based on the aerodynamic loading, the composite material was developed. The optimal material features a layup of epoxy and EGlass. With sufficient strength, the EGlass-Epoxy composite costs approximately $710 per blade for a total cost of $2840 per 4 blade turbine. Additionally, the weight of the material is approximately 20.4kgs per blade for a total of 81.6kgs per wind turbine.

The weight of the optimized support structure is 3.0385 kgs per strut. With the optimized composite material, the total cost of the support structure for the wind turbine is $784, each strut being $98 worth.

Based on these results, the final wind turbine farm consists of turbines constructed to the optimal dimensions with the EGlass-Epoxy composite at a spacing of 48 turbines per square mile.

8.2 Performance Results

While the optimization results provide the optimal theoretical design, is it necessary to weigh the results of each subsystem to understand the validity of the entire design. The best method to review the results is to examine the cost of wind turbines and the total power generated. The payback period of the system is essential to concluding if the design is a viable option.

$$P^* = 51.73\,W$$

$$Cost^* = \$3630$$

$$P_{48} = 2.48kW$$

$$Cost_{48} = \$174{,}240$$

Assuming the energy cost is fixed at its current rate of $0.0884 per kWh, the payback period for the wind turbines would be 16550 hours or 690 days (approx. 2 years). While this payback period is feasible it only accounts for the cost of the materials and not the operating cost, installation, and generator system. When accounting for these components, the payback period and power generation are far too low to serve as a reasonable option for energy production.

8.3 Project Conclusion

The results of the project confirm the initial assumption a wind farm given the wind conditions is not viable. The average wind speed is too low to produce the power necessary to payback the total cost of the wind turbine even with the optimal design. However, given a higher average wind speed, the implementation of the wind turbine optimized through this study would be viable. At an average wind speed of 10m/s the wind turbine would be rated at 1.1kW; a reasonable production for a small scale, urban vertical axis wind turbine.

9. REFERENCES

[3.1] http://www.windpowerengineering.com/construction/vertical-axis-wind-turbines-vs-horizontal-axis-wind-turbines/

[3.2] http://www.usa.com/Mesa-az-weather.htm

[4.1] Optimal placement of horizontal axis wind turbines in a wind farm for maximum power generation using a genetic algorithm by Xiaomin Chen, Ramesh Agarwal, 2005

[4.2] Manwell J.F., Mcgowan J.G. and Rogers A.L.. Wind Energy Explained. Wiley, 2009, pp. 146-151.

[4.3] Wind Turbine Placement in a wind farm using viral based optimization by Carlos M. Ituarte-Villarreal and Jose F. Espiritu

[4.4] Grady S.A., Hussaini M.Y., Abdulla M.M.. Placement of Wind Turbines Using Genetic Algorithms. Renewable Energy. Vol. 30, pp. 259-270, 2005.

[4.5] Mosetti G., Poloni C., Diviacco B.. Optimization of Wind Turbine Positioning in Large Wind Farms by Means of a Genetic Algorithm. J. of Wind Engineering and Aerodynamics. Vol. 51, pp. 105-116, 1994.

[4.6] Jacobs E.N. and Sherman A. Airfoil Section Characteristics as affected by Variations of the Reynolds Number. NACA Report 586, 1937.

[4.7] Werle M.J.. A New Analytical Model for Wind Turbine Wakes. Report No. FD 200801, Flodesign Inc., Wilbraham, MA, June 2008.

[4.8] Goldberg D.E.. Genetic Algorithms in Search, Optimization & Machine Learning. Addison-Wesley, 1989

[5.1] Patel, P. D.; Patel, D., An Analysis and Optimization of Mechanical Properties to Prolonged Service Life of Horizontal Axis Wind Turbine Blade 2014, 1 (6), 152–157.

[5.2] Rashedi, A.; Sridhar, I.; Tseng, K. J. Mater. Des. 2012, 37 (January 2016), 521–532.

[5.3] Islam, M.; Ahmed, F. U.; Ting, D. S.-K.; Fartaj, A. 1–11.

[5.4] Ancona, D.; McVeigh, J. Princet. Energy Resour. Int. LLC 2001, 1–8.

[5.5] Thirumalai, D. P. R. Int. J. Mater. Eng. Innov. 2014, 5 (2), 81.

[5.6] P. J. Schubel and R. J. Crossley, “Wind Turbine Blade Design,” pp. 3425–3449, 2012.

[5.7] “Laminate Analysis – Stiffness,” pp. 1–15.

[5.8] C. D. Section and R. Number, “Composite design Section 2 of 3 : Composite design guidelines,” no. October, 2011.

[5.9] T. D. Canonsburg, “ANSYS Composite PrepPost User ’ s Guide,” vol. 15317, no. November, pp. 724–746, 2013.

[5.10] G. Bohling, “C&PE 940, 19 October 2005,” no. October, pp. 1–20, 2005.

[5.11] “Response surface methodology,” 1996.

[5.12] X. Li, “18-660 : Numerical Methods for Engineering Design and Optimization,” pp. 1–19.

[5.13] http://www.pyopt.org/reference/optimizers.nlpql.html

[6.1] Malael, I., Dumitrescu, H., & Cardos, V. (2014). Numerical Simulation of Vertical Axis Wind Turbines at Low Tip Speed Ratios. Global Journal of Researches in Engineering: Numerical Methods, 14(1).

[6.2] Kozak, P. (2015). Two-Dimensional Optimization Methods of Vertical-Axis Wind Turbines.

[6.3] Carrigan, T. J., Dennis, B. H., Han, Z. X., & Wang, B. P. (2012). Aerodynamic Shape Optimization of a Vertical-Axis Wind Turbine Using Differential Evolution. ISRN Renewable Energy, 2012, 16.

[6.4] Rossander, M. (2015). Evaluation of Blade Force Measurement System for a Vertical Axis Wind Turbine Using Load Cells. Energies, 8, 5973–5996.

[6.5] Rathi, D. (2012). Performance Prediction and Dynamic Model Analysis of Vertical Axis Wind Turbine Blades with Aerodynamically Varied Blade Pitch. Raleigh.

[6.6] Wind Energy Technology. (n.d.). Honolulu.

[6.7] Brusca, S., Lanzafame, R., & Messina, M. (2014). Design of a Vertical-Axis Wind Turbine: How the Aspect Ratio Affects the Turbine's Performance. International Journal of Energy and Environmental Engineering, (5), 333–340.

[6.8] Ragheb, M. (2014). Optimal Rotor Tip Speed Ratio.

[6.9] Phoenix Metro Macroburst. (2016).

[6.10] Sheldahl, R. E., & Klimas, P. C. (1981). Aerodynamic Characteristics of Seven Symmetrical Airfoil Sections Through 180-Degree Angle of Attack for Use in Aerodynamic Analysis of Vertical Axis Wind Turbines.

[7.1] M. S. B. Eng, "Structural Optimization of Multi-Megawatt, Offshore Vertical Axis Wind Turbine Rotors - Identifying Structural Design Drivers and Scaling up of Vertical Axis Wind Turbine Rotors," pp. 1–182, 2013.

[7.2] B. Roscher, C. S. Ferreira, L. O. Bernhammer, H. A. Madsen, D. T. Griffith, and B. Stoevesandt, "Combined structural optimization and aeroelastic analysis of a Vertical Axis Wind Turbine," AIAA SciTech, no. January, pp. 1–10, 2015.

[7.3] Erik Andreassen, Ole Sigmund et. Al. "Efficient topology optimization in MATLAB using 88 lines of code", Structural and Multidisciplinary Optimization, 2010

10. APPENDIX A – OPTIMIZATION OF THE WIND FARM LAYOUT

```
%%%%%%%%%%%%%%%%%%%%%%%%%%%%%%%%%%%%%%%%%
%--Code developed by Sekar Sumanth D--%
%--Optimization of wind farm layout--%
%%%%%%%%%%%%%%%%%%%%%%%%%%%%%%%%%%%%%%%%%
function Xdisp = fun(x)
%-------Parameters------------%
%--Environment Parameters--%
rho    = 1.225;       %Density of air
U   = [26.5];         %Free stream velocity
efficiency =0.7;
%--Turbine parameters--%
Rr      = 1.5626;     %Raduis of the rotor
R    = Rr;

Lengthofblade= 1.4;   %Length of the blades
B      =4;            %Number of blades
H      = Lengthofblade*B;
```

```
c      =0.5;          %Chord length
lambda = 0.76;        %Tip speed ratio

%--Ratio of mean free stream velocity and velocity of in the wake--%
e= 0.887;

%--Radius of wake --%
adash  = 0.3330;
ro  = Rr* sqrt((1-adash)/(1-(2*adash)));
```

```
%-- Entrainment constant--%
zo    =0.3;
z     = H;
alpha = 0.5/(log(z/zo));
temp=(ro/alpha);


%--------Constraints-----------%
%Constraint 1: x(1) Number of Turbines required
%Constraint 2: x(2) Power output from single turbine
%Constraint 3: x(3) Axial induction factor

%-----Objective function-----%
Xdisp= abs(temp-temp*abs((((x(1)*efficiency*rho*R*H*4*(x(3))*((1-x(3))^2)*(U.^3))-
x(2))/(2*x(3)))));
%---------------------------------------------%
```

```
%--Non linear Constraints calculation--%
function [g,h] =NONLCON(x)

%--Inequality constraints--%
g =[(cost/(0.7*x(2)*x(1))-abs((x(1)*((2/3)+(1/3)*exp(-0.00174*x(1)^2))))); abs(x(3)-
abs(((1/16)*B*c*e*(18/pi)*(lambda/R))))];

%--Equaltity constrains--%
h= [abs(x(1)-abs((x(2)*x(3)*((1-x(3))^2*e))))];
```

```
%--Analysis file--%
options =optimset('Display','iter','LargeScale','off');
A=[];
b=[];
Aeq=[];
beq=[];

%--Lower bound and Upper bound--%
lb = [0,0,0];
ub = [100 100 100];

%--Initial Guess-%
```

```
x0 = [63,100,1];

%--Conversion factor--%
conversion = (3.28084*10^-5); % feet to meters
[xopt,fval,exitflag,output] =fmincon('fun',x0,A,b,Aeq,beq,lb,ub,'NONLCON')
minimumrequiredxvalue=(conversion)*fval
```

11. APPENDIX B - AERODYNAMIC SUBSYSTEM MATLAB CODE

VAWT_opt.m

```
%-------------------------------------------------------------------------
-----
%Matthew Brausch
%MAE 494: Design Optimization
%VAWT Optimization Project
%-------------------------------------------------------------------------
-----
clear

%Load Coefficient Data
NACA0012=xlsread('Coefficient Data 3.xlsx','NACA 0012 Coefficients');
NACA0012=[-flipud(NACA0012(2:length(NACA0012),:)) ;NACA0012];

NACA0015=xlsread('Coefficient Data 3.xlsx');
NACA0015=[-flipud(NACA0015(2:length(NACA0015),:)); NACA0015];

NACA0018=xlsread('Coefficient Data 3.xlsx','NACA 0018 Coefficients');
NACA0018=[-flipud(NACA0018(2:length(NACA0018),:)); NACA0018];

NACA0021=xlsread('Coefficient Data 3.xlsx','NACA 0021 Coefficients');
NACA0021=[-flipud(NACA0021(2:length(NACA0021),:)); NACA0021];

NACA0025=xlsread('Coefficient Data 3.xlsx','NACA 0025 Coefficients');
NACA0025=[-flipud(NACA0025(2:length(NACA0025),:)); NACA0025];

%Defining the Constant Parameters
v_inf=1; %Average wind speed for Mesa 8mph=~3.58m/s
rho_air=1.223; %General air density (kg/m^3)

%Approximating polynomial fits for drag and lift coefficients from -90
to
%90 degrees

%NACA 0012 coefficient polynomials
pl12=polyfit(NACA0012(:,1),NACA0012(:,2),5);
pd12=polyfit(NACA0012(:,1),NACA0012(:,3),5);
%Polynomial a function of angle of attack in degrees
```

```
Cl12=@(a)
pl12(1)*a^5+pl12(2)*a^4+pl12(3)*a^3+pl12(4)*a^2+pl12(5)*a+pl12(6);
Cd12=@(a)
pd12(1)*a^5+pd12(2)*a^4+pd12(3)*a^3+pd12(4)*a^2+pd12(5)*a+pd12(6);

%NACA 0015 coefficient polynomials
pl15=polyfit(NACA0015(:,1),NACA0015(:,2),5);
pd15=polyfit(NACA0015(:,1),NACA0015(:,3),5);
%Polynomial a function of angle of attack in degrees
Cl15=@(a)
pl15(1)*a^5+pl15(2)*a^4+pl15(3)*a^3+pl15(4)*a^2+pl15(5)*a+pl15(6);
Cd15=@(a)
pd15(1)*a^5+pd15(2)*a^4+pd15(3)*a^3+pd15(4)*a^2+pd15(5)*a+pd15(6);

%NACA 0018 coefficient polynomials
pl18=polyfit(NACA0018(:,1),NACA0018(:,2),5);
pd18=polyfit(NACA0018(:,1),NACA0018(:,3),5);
%Polynomial a function of angle of attack in degrees
Cl18=@(a)
pl18(1)*a^5+pl18(2)*a^4+pl18(3)*a^3+pl18(4)*a^2+pl18(5)*a+pl18(6);
Cd18=@(a)
pd18(1)*a^5+pd18(2)*a^4+pd18(3)*a^3+pd18(4)*a^2+pd18(5)*a+pd18(6);

%NACA 0021 coefficient polynomials
pl21=polyfit(NACA0021(:,1),NACA0021(:,2),5);
pd21=polyfit(NACA0021(:,1),NACA0021(:,3),5);
%Polynomial a function of angle of attack in degrees
Cl21=@(a)
pl21(1)*a^5+pl21(2)*a^4+pl21(3)*a^3+pl21(4)*a^2+pl21(5)*a+pl21(6);
Cd21=@(a)
pd21(1)*a^5+pd21(2)*a^4+pd21(3)*a^3+pd21(4)*a^2+pd21(5)*a+pd21(6);

%NACA 0025 coefficient polynomials
pl25=polyfit(NACA0025(:,1),NACA0025(:,2),5);
pd25=polyfit(NACA0025(:,1),NACA0025(:,3),5);
%Polynomial a function of angle of attack in degrees
Cl25=@(a)
pl25(1)*a^5+pl25(2)*a^4+pl25(3)*a^3+pl25(4)*a^2+pl25(5)*a+pl25(6);
Cd25=@(a)
pd25(1)*a^5+pd25(2)*a^4+pd25(3)*a^3+pd25(4)*a^2+pd25(5)*a+pd25(6);

%Unknown Coefficients:
%x(1)=chord length(m)
%x(2)=blade height(m)
%x(3)=tip speed ratio
%x(4)=aspect ratio (h/r)

%Function for the angle of attack and square of relative velocity
attack=@(theta,x) atand(sind(theta)/(x+cosd(theta)));
v_rel=@(theta,x) (v_inf*(1+x*cosd(theta)))^2+(v_inf*x*sind(theta))^2;

%Combined functions for the tangetial coefficient
```

```
Ct12=@(theta,x) Cl12(attack(theta,x))*sind(attack(theta,x))-...
    Cd12(attack(theta,x))*cosd(attack(theta,x));
Ct15=@(theta,x) Cl15(attack(theta,x))*sind(attack(theta,x))-...
    Cd15(attack(theta,x))*cosd(attack(theta,x));
Ct18=@(theta,x) Cl18(attack(theta,x))*sind(attack(theta,x))-...
    Cd18(attack(theta,x))*cosd(attack(theta,x));
Ct21=@(theta,x) Cl21(attack(theta,x))*sind(attack(theta,x))-...
    Cd21(attack(theta,x))*cosd(attack(theta,x));
Ct25=@(theta,x) Cl25(attack(theta,x))*sind(attack(theta,x))-...
    Cd25(attack(theta,x))*cosd(attack(theta,x));

%Initializing force functions
sum12=@(x) 0;
sum15=@(x) 0;
sum18=@(x) 0;
sum21=@(x) 0;
sum25=@(x) 0;

%Creating the summation portion of the force function
for i=0:5:360
    sum12=@(x) sum12(x)+Ct12(i,x)*v_rel(i,x);
    sum15=@(x) sum15(x)+Ct15(i,x)*v_rel(i,x);
    sum18=@(x) sum18(x)+Ct18(i,x)*v_rel(i,x);
    sum21=@(x) sum21(x)+Ct21(i,x)*v_rel(i,x);
    sum25=@(x) sum25(x)+Ct25(i,x)*v_rel(i,x);
end

%Averaged force function for 1 rotation
fun12=@(x) .5*(1/73)*rho_air*x(1)*x(2)*sum12(x(3));
fun15=@(x) .5*(1/73)*rho_air*x(1)*x(2)*sum15(x(3));
fun18=@(x) .5*(1/73)*rho_air*x(1)*x(2)*sum18(x(3));
fun21=@(x) .5*(1/73)*rho_air*x(1)*x(2)*sum21(x(3));
fun25=@(x) .5*(1/73)*rho_air*x(1)*x(2)*sum25(x(3));

%number of blades
n=4;

%Coefficient of performance function
COP12=@(x) -
n*fun12(x)*v_inf*x(3)/(.5*rho_air*2*(1/x(4))*x(2)^2*v_inf^3);
COP15=@(x) -
n*fun15(x)*v_inf*x(3)/(.5*rho_air*2*(1/x(4))*x(2)^2*v_inf^3);
COP18=@(x) -
n*fun18(x)*v_inf*x(3)/(.5*rho_air*2*(1/x(4))*x(2)^2*v_inf^3);
COP21=@(x) -
n*fun21(x)*v_inf*x(3)/(.5*rho_air*2*(1/x(4))*x(2)^2*v_inf^3);
COP25=@(x) -
n*fun25(x)*v_inf*x(3)/(.5*rho_air*2*(1/x(4))*x(2)^2*v_inf^3);

vol_max=0.25; %flat volume max

OF12=@(x) COP12(x)*(x(1)^2*x(2)*0.12/vol_max-1);
```

```
OF15=@(x) COP15(x)*(x(1)^2*x(2)*0.15/vol_max-1);
OF18=@(x) COP18(x)*(x(1)^2*x(2)*0.18/vol_max-1);
OF21=@(x) COP21(x)*(x(1)^2*x(2)*0.21/vol_max-1);
OF25=@(x) COP25(x)*(x(1)^2*x(2)*0.25/vol_max-1);

%Constraints and initial conditions for optimization
%Unknown Coefficients:
%x(1)=chord length(m)
%x(2)=blade height(m)
%x(3)=tip speed ratio
%x(4)=aspect ratio (h/r)

A=[-1, 0, 0, 0;... % c>0
    1, -1, 0, 0;... % h-c>0 c-h<0
    0, 1, 0, 0;... %h<5
    0, 0, -1, 0;... %tsr>0.1
    0, 0, 1, 0;... %tsr<8
    0, 0, 0, -1;... %AR>0.1
    0, 0, 0, 1]; %AR<2

%Inequality constraints
b=[0, 0, 5, 0.1, 8, 0.1, 2];

%Adding nonlinear constraints
nonlcon=@nlconstraints;

%Initial guess and limits
x0=[0.5, 1.5, 1.5, 0.5];
lb=[-1000, -1000, -1000, -1000];
up=[1000, 1000, 1000, 1000];

%Unused equality constraints
Aeq=[];
beq=[];

%Setting the fmincon solver to SQP
options=optimoptions('fmincon','Algorithm','sqp');

%Optimal values of c, h, tsr, and AR
x_opt(1,:)=fmincon(OF12,x0,A,b,Aeq,beq,lb,up,nonlcon);
x_opt(2,:)=fmincon(OF15,x0,A,b,Aeq,beq,lb,up,nonlcon);
x_opt(3,:)=fmincon(OF18,x0,A,b,Aeq,beq,lb,up,nonlcon);
x_opt(4,:)=fmincon(OF21,x0,A,b,Aeq,beq,lb,up,nonlcon);
x_opt(5,:)=fmincon(OF25,x0,A,b,Aeq,beq,lb,up,nonlcon);

cp=-[COP12(x_opt(1,:)); COP15(x_opt(2,:)); COP18(x_opt(3,:)); ...
    COP21(x_opt(4,:)); COP25(x_opt(5,:))];
f=-[OF12(x_opt(1,:)); OF15(x_opt(2,:)); OF18(x_opt(3,:));...
    OF21(x_opt(4,:)); OF25(x_opt(5,:))];

hold on
grid on
```

```
OF25plot=@(x) -OF25([x_opt(5,1),x_opt(5,2),x_opt(5,3),x]);
ezplot(OF25plot,[0.5,1.5])
scatter(x_opt(:,4),f)
xlabel('Chord Length (m)')
ylabel('Objective  Function')
```

nlconstraints.m

```
%Function of nonlinear constraints for optimization
function [c, ceq]=nlconstraints(x)
c=[-4*x(1)/(2*x(2)*(1/x(4))),... %solidity>0
    4*x(1)/(2*x(2)*(1/x(4)))-2,... %solidity<2
    -x(3)*3.58*x(2)/(x(4)),... %omega>0
    x(3)*3.58*x(2)/(x(4))-20,... %omega<10
    -x(1)*x(2),... %area>0
    x(1)*x(2)-1,... %area<1
    -x(2)/x(4),... %radius>0
    x(2)/x(4)-2.5];... %radius<2.5
ceq=[];
end
```

12. APPENDIX C – MATLAB CODE FOR MATERIAL PROPERTY CALCULATION

```
%% MATLAB CODE FOR MATERIAL PROPERTY CALCULATION
% Adithya Lakkur Venugopal
% MAE 598 Design Optimization
% OPTIMIZATION OF VERTICAL AXIS WIND TRUBINE

%% Composite Material 1
%Glass reinforced plastic
%Matrix - Epoxy ; Reinforcement/Fiber - E Glass

%Matrix - Epoxy Properties
density_epoxy = 1350;    %Density of Epoxy in kg/m3
E_epoxy = 3.59*10^9;     %Young's Modulus in N/m2
G_epoxy = 4.4*10^9;      %Rigidity Modulus in N/m2
C_epoxy = 11;          %Cost per kg

%Reinforcement/Fiber - E Glass Properties
density_eglass = 2575;   %Density of EGlass in kg/m3
E_eglass = 72.4*10^9;    %Young's Modulus in N/m2
G_eglass = 33*10^9;      %Rigidity Modulus in N/m2
C_eglass = 12;        %Cost per kg

v1_fiber = [0.35, 0.4, 0.45, 0.5, 0.55];
v1_matrix = zeros(1,5);
```

```
for i = 1:length(v1_fiber)
    b = 1 - v1_fiber(i);
    v1_matrix(i) = v1_matrix(i) + b;
end

%% Young's Modulus & Density of the composite in longitudional loading
%Density of the composite in longitudional loading
density_c_l = (density_epoxy*v1_matrix) + (density_eglass*v1_fiber);

%Young's Modulus of the composite in longitudional loading
E1_c_1 = (E_epoxy*v1_matrix) + (E_eglass*v1_fiber);

%% Young's Modulus & Density of the composite in transverse loading
%Density of the composite in transverse loading remains the same

%Young's Modulus of the composite in transverse loading
e2 = (v1_matrix/E_epoxy) + (v1_fiber/E_eglass);
E2_c_1 = 1./e2;

%% Rigidity Modulus of the composite
g12 = (v1_matrix/G_epoxy) + (v1_fiber/G_eglass);
G12_c_1 = 1./g12;

%% Poisson's ratio along the longitudional & transverse direction

v12_c_1 = [0.35 0.35 0.35 0.35 0.35];   %Assuming the poisson's ratio along
the longitudional

%Poisson's ratio along transverse direction
v21_c_1 = (E2_c_1.*(v12_c_1))./E1_c_1;

%% Calculating the cost of the composite ($/kg)
C_composite_1 = zeros(1,5);
for j = 1:5
    C_composite_1(j) = C_epoxy + (C_eglass - C_epoxy) * (density_eglass *
v1_fiber(j)/(density_c_l(j)));
end

% Cost per unit modulus per unit mass ($/(GPa*kg))
C_composite_1M = zeros(1,5);
for k = 1:5
    C_composite_1M(k) = (10^9)*(C_composite_1(k)/E1_c_1(k));
end


%Composite Material 2
%Carbon Fiber Reinforcement Plastic
%Matrix - Epoxy ; Reinforcement/Fiber - Carbon fiber (IM6)

%Matrix - Epoxy Properties
density_epoxy3 = 1250;     %Density of Vinyl Ester in kg/m3
E_epoxy3 = 3.21*10^9;      %Young's Modulus in N/m2
G_epoxy3 = 1.019*10^9;     %Rigidity Modulus in N/m2
C_epoxy3 = 22.01;          %Cost per kg
```

```
%Reinforcement/Fiber - Carbon fiber (IM6) Properties
density_carbon = 1740;      %Density of Vinyl Ester in kg/m3
E_carbon = 276*10^9;        %Young's Modulus in N/m2
G_carbon = 18*10^9;         %Rigidity Modulus in N/m2
C_carbon = 88.18;           %Cost per kg

v3_fiber = [0.35, 0.4, 0.45, 0.5, 0.55];
v3_matrix = zeros(1,5);
for i = 1:length(v3_fiber)
    b = 1 - v3_fiber(i);
    v3_matrix(i) = v3_matrix(i) + b;
end

%% Young's Modulus & Density of the composite in longitudional loading
%Density of the composite in longitudional loading
density_c_3 = (density_epoxy3*v3_matrix) + (density_carbon*v3_fiber);

%Young's Modulus of the composite in longitudional loading
E1_c_3 = (E_epoxy3*v3_matrix) + (E_carbon*v3_fiber);

%% Young's Modulus & Density of the composite in transverse loading
%Density of the composite in transverse loading remains the same

%Young's Modulus of the composite in transverse loading
e2_composite_3 = (v3_matrix/E_epoxy3) + (v3_fiber/E_carbon);
E2_c_3 = 1./e2_composite_3;

%% Rigidity Modulus of the composite
g12_composite_3 = (v3_matrix/G_epoxy3) + (v3_fiber/G_carbon);
G12_c_3 = 1./g12_composite_3;
%% Poisson's ratio along the longitudional & transverse direction

v12_c_3 = [0.25 0.25 0.25 0.25 0.25];   %Assuming the poisson's ratio along
the longitudional

%Poisson's ratio along transverse direction
v21_c_3 = (E2_c_3.*(v12_c_3))./E1_c_3;

%% Calculating the cost of the composite ($/kg)
C_composite_3 = zeros(1,5);
for j = 1:5
    C_composite_3(j) = C_epoxy3 + (C_carbon - C_epoxy3) * (density_carbon *
v3_fiber(j)/(density_c_3(j)));
end

% Cost per unit modulus per unit mass ($/(GPa*kg))
C_composite_3M = zeros(1,5);
for k = 1:5
    C_composite_3M(k) = (10^9)*(C_composite_3(k)/E1_c_3(k));
end
```

13. APPENDIX D – TOPOLOGY OPTIMIZATION TOP88 CODE MODIFIED

```
%%%% AN 88 LINE TOPOLOGY OPTIMIZATION CODE Nov, 2010 %%%%
function top88(nelx,nely,volfrac,penal,rmin,ft)
%% MATERIAL PROPERTIES
E0 = 1;
Emin = 1e-9;
nu = 0.3;

mel = 30/nelx/nely;
w = 1.5;
g = 9.8;
nl = 0.5/nelx;


%% PREPARE FINITE ELEMENT ANALYSIS
A11 = [12  3 -6 -3;  3 12  3  0; -6  3 12 -3; -3  0 -3 12];
A12 = [-6 -3  0  3; -3 -6 -3 -6;  0 -3 -6  3;  3 -6  3 -6];
B11 = [-4  3 -2  9;  3 -4 -9  4; -2 -9 -4 -3;  9  4 -3 -4];
B12 = [ 2 -3  4 -9; -3  2  9 -2;  4  9  2  3; -9 -2  3  2];
KE = 1/(1-nu^2)/24*([A11 A12;A12' A11]+nu*[B11 B12;B12' B11]);
nodenrs = reshape(1:(1+nelx)*(1+nely),1+nely,1+nelx);
edofVec = reshape(2*nodenrs(1:end-1,1:end-1)+1,nelx*nely,1);
edofMat = repmat(edofVec,1,8)+repmat([0 1 2*nely+[2 3 0 1] -2 -
1],nelx*nely,1);
iK = reshape(kron(edofMat,ones(8,1))',64*nelx*nely,1);
jK = reshape(kron(edofMat,ones(1,8))',64*nelx*nely,1);
% DEFINE LOADS AND SUPPORTS (HALF MBB-BEAM)
F = sparse(2,1,-1,2*(nely+1)*(nelx+1),1);

%%%%%%%%%%%%%%%%%%%%%%%%%%%%%%%%%%%%%%%%%%%%%%%%%%%%%%%%%%%%
for i = 1:(nelx+1)
    F((1:2:((nely+1)*2))+(i-1)*(nely+1)*2) = -mel*w^2*((nelx+1-i)*nl);
    F((2:2:((nely+1)*2))+(i-1)*(nely+1)*2) = -mel*g;
end
F((nely+1)*2+(nelx)*(nely+1)*2) = -2.5*1451+F((nely+1)*2+(nelx)*(nely+1)*2);
%%%%%%%%%%%%%%%%%%%%%%%%%%%%%%%%%%%%%%%%%%%%%%%%%%%%%%%%%%%%

U = zeros(2*(nely+1)*(nelx+1),1);
fixeddofs = [(1:2*(nely+1))+nelx*(nely+1)*2];
% fixeddofs = union([1:2:2*(nely+1)],[2*(nelx+1)*(nely+1)]);
alldofs = [1:2*(nely+1)*(nelx+1)];
freedofs = setdiff(alldofs,fixeddofs);
%% PREPARE FILTER
iH = ones(nelx*nely*(2*(ceil(rmin)-1)+1)^2,1);
jH = ones(size(iH));
sH = zeros(size(iH));
```

```
k = 0;
for i1 = 1:nelx
  for j1 = 1:nely
    e1 = (i1-1)*nely+j1;
    for i2 = max(i1-(ceil(rmin)-1),1):min(i1+(ceil(rmin)-1),nelx)
      for j2 = max(j1-(ceil(rmin)-1),1):min(j1+(ceil(rmin)-1),nely)
        e2 = (i2-1)*nely+j2;
        k = k+1;
        iH(k) = e1;
        jH(k) = e2;
        sH(k) = max(0,rmin-sqrt((i1-i2)^2+(j1-j2)^2));
      end
    end
  end
end
H = sparse(iH,jH,sH);
Hs = sum(H,2);
%% INITIALIZE ITERATION
x = repmat(volfrac,nely,nelx);
xPhys = x;
loop = 0;
change = 1;
%% START ITERATION
while change > 0.01
  loop = loop + 1;
  %% FE-ANALYSIS
  sK = reshape(KE(:)*(Emin+xPhys(:)'.^penal*(E0-Emin)),64*nelx*nely,1);
  K = sparse(iK,jK,sK); K = (K+K')/2;
  U(freedofs) = K(freedofs,freedofs)\F(freedofs);
  %% OBJECTIVE FUNCTION AND SENSITIVITY ANALYSIS
  ce = reshape(sum((U(edofMat)*KE).*U(edofMat),2),nely,nelx);
  c = sum(sum((Emin+xPhys.^penal*(E0-Emin)).*ce));
  dc = -penal*(E0-Emin)*xPhys.^(penal-1).*ce;
  dv = ones(nely,nelx);
  %% FILTERING/MODIFICATION OF SENSITIVITIES
  if ft == 1
    dc(:) = H*(x(:).*dc(:))./Hs./max(1e-3,x(:));
  elseif ft == 2
    dc(:) = H*(dc(:)./Hs);
    dv(:) = H*(dv(:)./Hs);
  end
  %% OPTIMALITY CRITERIA UPDATE OF DESIGN VARIABLES AND PHYSICAL DENSITIES
  l1 = 0; l2 = 1e9; move = 0.2;
  while (l2-l1)/(l1+l2) > 1e-3
    lmid = 0.5*(l2+l1);
    xnew = max(0,max(x-move,min(1,min(x+move,x.*sqrt(-dc./dv/lmid)))));
    if ft == 1
      xPhys = xnew;
    elseif ft == 2
      xPhys(:) = (H*xnew(:))./Hs;
    end
    if sum(xPhys(:)) > volfrac*nelx*nely, l1 = lmid; else l2 = lmid; end
  end
  change = max(abs(xnew(:)-x(:)));
  x = xnew;
  %% PRINT RESULTS
  fprintf(' It.:%5i Obj.:%11.4f Vol.:%7.3f ch.:%7.3f\n',loop,c, ...
```

```
    mean(xPhys(:)),change);
  %% PLOT DENSITIES
  colormap(gray); imagesc(1-xPhys); caxis([0 1]); axis equal; axis off;
drawnow;
end
%
%%%%%%%%%%%%%%%%%%%%%%%%%%%%%%%%%%%%%%%%%%%%%%%%%%%%%%%%%%%%%%%%%%%%%%%%%%%%%%%
% This Matlab code was written by E. Andreassen, A. Clausen, M. Schevenels,%
% B. S. Lazarov and O. Sigmund,  Department of Solid  Mechanics,           %
%  Technical University of Denmark,                                        %
%  DK-2800 Lyngby, Denmark.                                                %
% Please sent your comments to: sigmund@fam.dtu.dk                         %
%                                                                          %
% The code is intended for educational purposes and theoretical details    %
% are discussed in the paper                                               %
% "Efficient topology optimization in MATLAB using 88 lines of code,       %
% E. Andreassen, A. Clausen, M. Schevenels,                                %
% B. S. Lazarov and O. Sigmund, Struct Multidisc Optim, 2010               %
% This version is based on earlier 99-line code                            %
% by Ole Sigmund (2001), Structural and Multidisciplinary Optimization,    %
% Vol 21, pp. 120--127.                                                    %
%                                                                          %
% The code as well as a postscript version of the paper can be             %
% downloaded from the web-site: http://www.topopt.dtu.dk                   %
%                                                                          %
% Disclaimer:                                                              %
% The authors reserves all rights but do not guaranty that the code is     %
% free from errors. Furthermore, we shall not be liable in any event       %
% caused by the use of the program.                                        %
%%%%%%%%%%%%%%%%%%%%%%%%%%%%%%%%%%%%%%%%%%%%%%%%%%%%%%%%%%%%%%%%%%%%%%%%%%%%%%%
```